Wnt/β-catenin signalling inhibits T-type calcium channels in cardiomyocytes

By

Kaya Florczak

Thesis submitted to the University of Ottawa in partial fulfillment of the requirements for the Degree of:

Master of Science in Cellular and Molecular Medicine

Department of Cellular and Molecular Medicine

Faculty of Medicine

University of Ottawa

Abstract

Background: The Wnt/β-catenin signalling pathway is activated in arrhythmogenic heart diseases such as myocardial infarction and heart failure, but it is unclear if the pathway regulates cardiac ion channels and thus may play a role in arrhythmogenesis. Previous PCR array screening from our lab showed that the transcript level of the T-type calcium channel gene *Cacna1g* was reduced in primary culture of neonatal rat ventricular myocytes (NRVMs) after activation of Wnt/β-catenin signalling with Wnt3a protein (100 ng/ml) or a small molecule activator of the pathway, CHIR (3 μM) ($n=3$, $p<0.01$). In this study, we examined the effects of Wnt/β-catenin signalling on T-type calcium channels ($Ca_v3.1$), which play a key role in the pacemaker function of the sinoatrial node (SAN).

Results: RT-qPCR and western blot demonstrated dose-dependent reductions in *Cacna1g* mRNA ($n=7$, $p<0.01$) and $Ca_v3.1$ protein ($n=4$, $p<0.01$) in NRVMs after treatment with CHIR (3 μM). There was also a decrease in *Cacna1g* mRNA in human induced pluripotent stem cell-derived cardiomyocytes (hiPSC-CMs) after treatment with CHIR (5 μM) ($n=4$; $p<0.001$). Patch-clamp recording demonstrated reduced T-type calcium current ($I_{Ca,T}$) in NRVMs after Wnt3a treatment (300 ng/ml) ($n=5$, $p<0.05$). In isolated mouse SAN tissue, perfusion with an $I_{Ca,T}$ blocker, ML-218 (3-30 μM), led to dose-dependent reductions in spontaneous beating rate ($n=4$, $p<0.0001$) indicating a critical role of $I_{Ca,T}$ in SAN pacemaking. In adult rats, activation of Wnt/β-catenin signalling through the application of CHIR in a poloxamer gel to the SAN region did not alter the in vivo heart rate in electrocardiogram (ECG) ($n=8$, $p=0.12$). However, ex vivo culture of SAN tissue from the in vivo experiments revealed that intrinsic beating rate was reduced in the CHIR treated group ($n=7$) compared to the control (DMSO) ($n=8$) ($p<0.05$).

Summary: Wnt/β-catenin signalling inhibits T-type Ca^{2+} current in cardiomyocytes by, at least partly, reduced *Cacna1g* mRNA and $Ca_v3.1$ protein. Activation of Wnt/β-catenin signalling reduces the intrinsic heart rate likely by inhibition of T-type Ca^{2+} current in SAN pacemaker cells.

Keywords: Wnt/β-catenin signalling pathway, T-type calcium channels, Sinoatrial node

Acknowledgements

First and foremost, I would like to express my sincere gratitude to my advisors, Dr. Wenbin Liang and Dr. Darryl Davis, for their continuous support of my M.Sc. research and study, as well as their patience, motivation, enthusiasm, and immense knowledge. Their guidance helped me immeasurably through all the time researching and writing this thesis. It was an honor to have the opportunity to work in their labs. Besides my advisors, I would also like to thank the rest of my thesis committee: including Dr. Frans Leenen and Dr. Alex Stewart for their encouragement, helpful comments, and challenging questions.

My sincerest thanks goes to my fellow labmate and mentor, Dr. Alice Lu, who guided me in all my research endeavors and provided valuable insight when I needed it most. Furthermore, I am grateful to my successors, including M.Sc. student Jerry Wang, for taking over experiments and expressing such enthusiasm in doing so.

Last, but not least, I would like to thank my parents, Michele and Derek Gaudet, for making education such an important part of my life and supporting me endlessly in every new venture. Above all, the love of my life, Cameron, whom I had the honor of marrying while working on this project; thank you for your understanding of the demands of graduate school, for being my sounding board, for helping me rehearse my presentations, and for always encouraging me to achieve my goals.

Table of Contents

List of Abbreviations

α-SMA – Alpha smooth muscle actin

AC – Adenylyl cyclase

AcH – Acetylcholine

ANS – Autonomic nervous system

APC – Adenomatous polyposis coli

ARVC – Arrhythmogenic right ventricular cardiomyopathy

AV – Atrioventricular

AVN – Atrioventricular node

Bpm – Beats per minute

CAD – Coronary artery disease

$Ca_v3.1$ – T-type calcium channel

CCS – Cardiac conduction system

CeOH – Cesium hydroxide

CHB – Congenital heart block

ChIP – Chromatin immunoprecipitation

CHIR – CHIR99021

CK-1 – Casein kinase 1

CO2 – Carbon dioxide

cSAN – Central sinoatrial node tissue

CsF – Cesium fluoride

CT – Cristae terminalis

CVD – Cardiovascular disease

Cx - Connexin

DMSO – Dimethylsulfoxide

DMEM – Dulbecco's Modified Eagle's Medium

DVL – Dishevelled protein

ECG – Electrocardiogram

ECM – Extracellular matrix

EGTA – Ethylene glycol tetraacetic acid

EMG – Electromyogram

EMT – Epithelial–mesenchymal transition

FA – Flecainide acetate

Fz – Frizzled receptor

GFP – Green fluorescent protein

G_i – Inhibitory G proteins

G_s – Stimulatory G proteins

GSK-3β – Glycogen synthase kinase 3 beta

HCN4 - Potassium/sodium hyperpolarization-activated cyclic nucleotide-gated channel 4

HEPES – Hydroxyethyl piperazineethanesulfonic acid

HF – Heart failure

hiPSC – Human induced pluripotent stem cell-derived cardiomyocytes

HRV – Heart rate variability

I_f – Funny channel current

$I_{Ca,L}$ – L-type calcium current

$I_{Ca,T}$ – T-type calcium current

If – Funny current

IVC – Inferior vena cava

LEF – Lymphoid enhancer-binding factor

Li^+ – Lithium ions

LP – Leading pacemaker

LRP 5/6 – Low-density lipoprotein receptor-related protein 5/6

M_2R – Muscarinic type 2 receptors

Mg-ATP – Adenosine triphosphate magnesium salt

ML-218 – Selective T-Type calcium channel inhibitor

ms – Milliseconds

Na-GTP – Guanosine triphosphate sodium salt

$Na_v1.5$ – Cardiac sodium channel

NE - Norepinephrine

NRSF - Neuron-restrictive silencer factor

NRVMs – Neonatal rat ventricular myocytes

PA – Pulmonary artery

PKA – Protein kinase A

pSAN – Peripheral sinoatrial node

PV – Pulmonary vein

RA – Right atrium

RNA – Ribonucleic acid

RT-qPCR – Real-time quantitative polymerase chain reaction

RV – Right ventricle

SAN – Sinoatrial node

SCN5A – Gene encoding $Na_v1.5$

SDRR – Standard deviation between R-R intervals

sFRP- Secreted Frizzled-related proteins

SND – Sinoatrial node dysfunction

SSS – Sick sinus syndrome

SVC – Superior vena cava

Tbx3 – T-box transcription factor 3

TCF – T-cell factor

Wnt – Wingless/Int-1 gene family

List of Figures

List of Tables

1. Introduction

1.1. Cardiac Conduction System

The heart is composed of chamber working myocytes that contract to propel blood in atria and ventricles, as well as specialized myocytes in the cardiac conduction system (CCS) that generate and conduct electrical impulses which control the rhythmic contractions of the chambers (Park & Fishman, 2011). The CCS is composed of 1) the sinoatrial node (SAN) that generates the electrical impulses, 2) the atrioventricular node (AVN), and 3) His bundle/branches and Purkinje fibers that relay the impulses to ventricular myocytes for coordinated excitation and contraction (Park & Fishman, 2011).

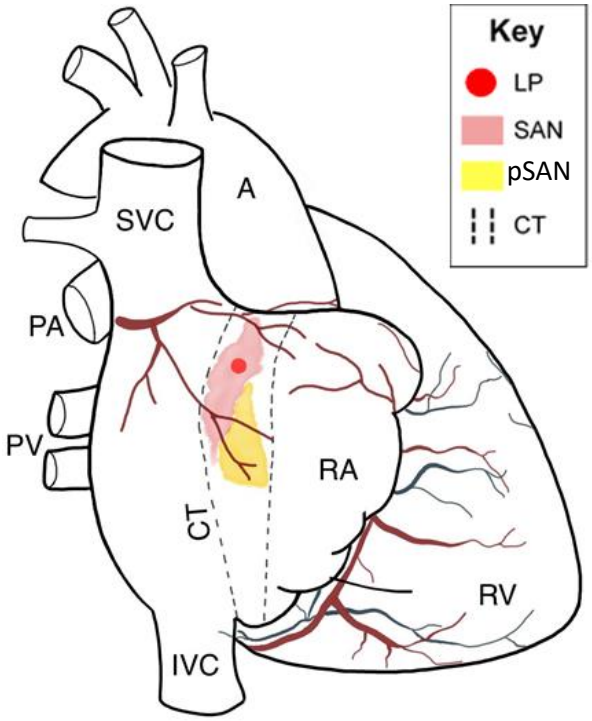

Figure 1: Model of the sinoatrial node. Approximate anatomical location and distribution of the lead pacemaker (LP) and peripheral sinoatrial node area (pSAN) in the right atrium (RA) of a human heart. Adapted from a mathematical model proposed by Chandler et al. (2011). SVC = superior vena cava; A = aorta; PA = pulmonary artery; PV = pulmonary vein; CT = cristae terminalis; IVC = inferior vena cava; RV = right ventricle. Heart adapted from AnatomyZone 3D heart model (http://www.anatomyzone.com). Nodal architecture based on Chandler et al. (2011) and Dobrzynski et al. (2005).

1.2. Sinoatrial Node

The sinoatrial node (SAN) is the primary pacemaker of mammalian hearts. It is a small, specialized structure located in the right atrium, below the superior vena cava (SVC) and lateral to the cristae terminalis (CT) (Figure 1). SAN pacemaker cells (SAN cells) can be identified by their spindle-like morphology and unique action potential profile (Figure 3). SAN cells have the property of automaticity due to an unstable resting membrane potential, which spontaneously depolarizes the membrane to threshold potential (around -40 mV) and generates rhythmic action potentials (Park & Fishman, 2011).

In 2005, Dobrinski et al. created the first three-dimensional anatomically detailed model of a rabbit SAN using histology, immunohistochemistry, and RNA isolation. This model revealed a 'leading pacemaker' (LP) area consisting of small cells in a mesh-like organization that did not express connexin 43 (Cx43). In the exit path from the SAN, they identified a peripheral area consisting of larger cells that did express Cx43 and were organized in a parallel fashion. In 2011, Chandler et al. used histology of human right atrial tissue preparations to create a mathematical model delineating the general SAN tissue from a distinct peripheral SAN region (pSAN) which was thought to play a critical role in propagation of action potentials from the central SAN to the right atrium (Figure 1).

There are unique ion channels that are predominantly expressed in the SAN and contribute to its pacemaking ability. SAN cell action potentials are separated into 3 phases (Phase 0, 4, and 3). A major ionic current that mediates automaticity in SAN cells is the funny current (I_f), which is mediated by a potassium/sodium hyperpolarization-activated cyclic nucleotide-gated channel 4 (HCN4). At maximum diastolic potential (-60 to -70 mV), when the cell is hyperpolarized, voltage dependent HCN4 is activated and allows the

influx of positive potassium (K^+) and sodium (Na^+) ions thereby initiating diastolic depolarization (Phase 4) of the SAN action potential.

In addition to I_f, a number of other ion channels play a role in pacemaker function. The heterogenous distribution of ion channels in the CCS (Figure 2) is indicative of the specific role of specialized subunits in initiating and propagating impulses. For example, the $Ca_V3.1$-mediated T-type calcium channels are highly expressed in the SAN (30-fold greater than in the atrium) and are absent in ventricular myocytes. It is befitting that these calcium channels are also known to contribute to phase 4 diastolic depolarization during the pacemaker potential in SAN cells (Schram, Pourrier, Melnyk & Nattel, 2002). There is also evidence of selective expression of T-type calcium channels along Purkinje fibers that contribute to calcium signalling within Purkinje cells during action potential propagation (Hildebrand et al., 2009).

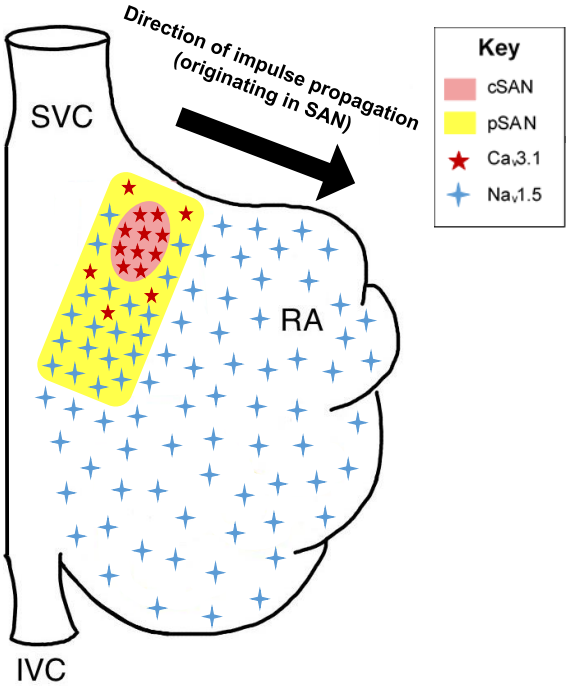

Figure 2: Heterogenous expression of ion channels in the right atrium. A diagram of the right atrium shows a representation of the patterned expression of T-type calcium channels and $Na_V1.5$ sodium channels that contribute to initiation and propagation of the sinoatrial node action potential. SVC = superior vena cava, CT = cristae terminalis, IVC = inferior vena cava, RA = right atrium, LP = lead pacemaker, pSAN = peripheral sinoatrial node area. Diagram based on literature for distribution patterns of $Ca_V3.1$ (Vassort, Talavera & Alvarez, 2006) and $Na_V1.5$ (Lei et al., 2004).

Furthermore, the $Na_v1.5$-mediated cardiac sodium channels, although absent in the center of the SAN, are expressed in the peripheral SAN (Figure 2) to allow rapid impulse propagation to the surrounding atrial tissues and atrioventricular node (AVN) (Monfredi et al., 2010; Park & Fishman, 2011).

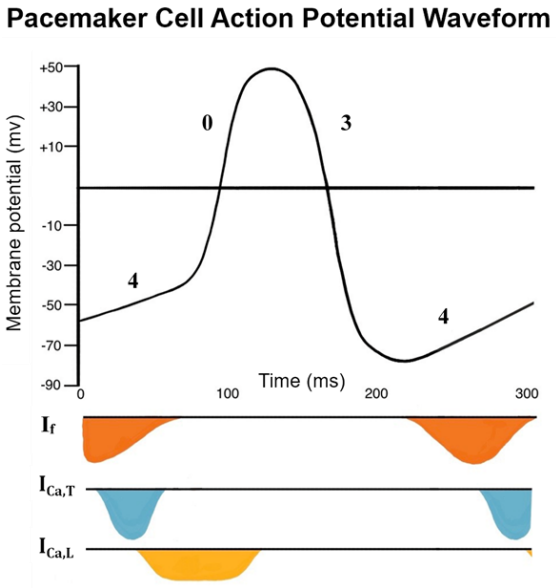

Figure 3: Ion channel activation patterns in sinoatrial node cells. The contribution of cardiac T-type calcium channels, L-type calcium channels, and funny channels displayed parallel to a sinoatrial node cell action potential waveform. I_f = funny channels, $I_{Ca,T}$ = T-type calcium channel, $I_{Ca,L}$ = L-type calcium channel, mv = millivolts, ms = milliseconds. Figure based on information presented in Cardiovascular Physiology Concepts Second Edition (Klabunde et al., 2012)

In Phase 4, at peak membrane depolarization (-70 to -60 mv), I_f channels slowly open, raising membrane potential. At approximately -55 to -50 mV, T-type calcium (Ca^{2+}) channels open. Together, Ca^{2+} and Na^+ ions depolarize the membrane to action potential threshold (-40 mV). At this higher membrane potential, T-type calcium channels inactivate, and L-type calcium channels open, leading to a rapid 'upstroke' of positive ion influx referred to as Phase 0 (Irisawa, Brown & Giles, 1993) (Figure 3).

Cardiomyocytes display an action potential plateau known as Phase 1 and 2, but when SANCs approach peak membrane potential around +50 mV, positive ion influx channels begin to close, and potassium (K^+) ions flow out of the cell initiating Phase 3 repolarization.

1.2.1. Sinoatrial Node Dysfunction

Abnormalities in the generation or conduction of the impulses disturb the normal heartbeat, leading to arrhythmias. Sinoatrial node dysfunction (SND), also called sick sinus syndrome (SSS), is caused by impaired impulse generation and/or conduction in the SAN, and can manifest as sinus pause/arrest, bradycardia, sinus-exit block, alternating tachy- and brady-cardia, and chronotropic incompetence. SND is often progressive, and patients can be asymptomatic in the early stages of disease (Wahls, 1985).

SND has a prevalence of ~535 cases per million in the general population but occurs in 1 of every 600 adults at ages of >65 years (Benjamin et al., 2017) and is responsible for ~50% of the electronic pacemaker implantations in Canada and the United States. Approximately half of all SND patients have tachy-brady syndrome, which is associated with a high risk for stroke and death (Benjamin et al., 2017). Although SND is primarily an age-related disease, it can be a consequence of cardiac remodeling during heart failure (Opthof et al., 2000; Chan et al., 2018).

SND is normally diagnosed using electrocardiogram (ECG) features of bradycardia (<60bpm) or asystolic pauses (>3 seconds), and the main causes of SND are commonly cited as fibrosis, cell loss, and coronary artery disease (Choudhury, Boyett, and Morris, 2015). However, SND is simply a phenotype that can be caused by many underlying pathologies including diabetes, exercise training, heart failure, ischemia, or ageing (Choudhury, Boyett, and Morris, 2015).

There is widespread electrical remodeling of the atria and SAN with ageing as a result of changes in expression of important ion channels involved in normal pacemaker

activity. For example, $Na_v1.5$ has been shown to decrease around the SAN in ageing rats which could lead to SAN exit block (Yanni et al., 2010). A comparison of young and old guinea pigs also showed a decline in levels of L-type calcium channel $Ca_v1.2$, which plays a key role in the phase 0 upstroke of the SAN action potential (Tellez et al., 2006).

Studies investigating familial SND have revealed underlying gene mutations that play a critical role in normal SAN pacemaking. Several point mutations or deletions within the HCN4 gene have been found to be associated with bradycardia or intermittent atrial fibrillation (Nof et al., 2007; Duhme et al., 2013). Mutations of the *SCN5A* gene that encodes $Na_v1.5$ can also lead to dysfunction in normal conduction in the SAN (Schulze-bahr et al., 2003; Milanesi et al., 2006).

Endurance athletes often exhibit sinus bradycardia as a result of significant exercise training (Baldesberger et al., 2008). While high vagal tone may contribute to lower resting heart rate, full autonomic blockade has also revealed lower intrinsic activity in athletes (Boyett et al., 1985). Rats and mice with training-induced bradycardia showed a downregulation of Hcn4 and Tbx3 (a transcription factor found selectively in the cardiac conduction system) compared with controls (D'Souza et al., 2014) suggesting electrical modeling as a mechanism for bradycardia in athletes. It is possible that these changes could be an early symptom of SND in athletes who require pacemaker implementation later in life (Choudhury, Boyett, and Morris, 2015).

While there are still many mechanisms, genes, and pathways to be explored in SAN research, ion channel remodeling is now thought to be a major contributor to SND, although the pattern of remodeling varies widely in different disease and is complex with many overlapping factors (Choudhury, Boyett, and Morris, 2015). Further investigation

into pacemaker-specific ion channels and how they may contribute to SAN function and dysfunction may help elucidate major factors underlying these disease processes.

1.3. Autonomic Nervous System

The autonomic nervous system (ANS) plays a role in cardiac physiology by tuning the automaticity of SAN cells and altering conduction rate through the AVN (Lakatta et al., 2010). The SAN is richly innervated by both the parasympathetic and the sympathetic nervous systems to alter pacemaker activity in response to stimuli. Parasympathetic input via the vagal nerve reduces SAN pacemaker activity and is the dominant input at rest in humans. Sympathetic nerve input and adrenal medullary release of catecholamines increase the sinus rate and is the dominant input at rest in murine animals (Lymperopoulos, Rengo, & Koch, 2013).

The sympathetic nervous system (SNS) has multiple projections that can influence cardiac function at the SAN or cardiomyocyte level primarily through the release of norepinephrine (NE) from the chain ganglia; superior, middle, and inferior cervical ganglia; or the adrenal medulla (Gordon, Gwathmey, & Xie, 2015). NE is chemically similar to epinephrine (i.e., adrenalin); sympathetic postganglionic fibers are also referred to as “adrenergic fibers”. In the heart, NE binds to β1-adrenergic receptors (β1-AR) located on the cell surface. In SAN cells, sympathetic stimulation results in positive chronotropic effect (increased heart rate). In cardiomyocytes, stimulation by the SNS increases intracellular calcium concentration and has a positive inotropic effect (increased contractility) in the atria and ventricles. SNS activity can also enhance conduction velocity in the AV node (positive dromotropic effect) (Gordon, Gwathmey, & Xie, 2015).

The sympathetic neurotransmitter NE (or other catecholamines) binds to β1-AR on the outside of the cell and binds stimulatory G proteins (G_s) to the receptor's intracellular domain. Guanosine triphosphate (GTP) displaces guanosine diphosphate (GDP) and activates the G_s. The activated G_s can then bind to and activate then adenylyl cyclase (AC), which catalyzes the conversion of ATP to cAMP, a powerful chemical messenger that can activate protein kinase A (pKA). In turn, pKA can phosphorylate multiple target proteins, such as L-type calcium channels. Phosphorylation of ion channels keeps them open longer, leading to greater influx of positive ions, more frequent depolarization events, and increased heart rate (Gordon, Gwathmey, & Xie, 2015).

Conversely, the parasympathetic nervous system (PNS) influences heart rate via acetylcholine (AcH) release from the vagus nerve. AcH binds to muscarinic type 2 receptors (M_2R) on the cell surface thereby activating intracellular inhibitory G proteins (G_i). There are 3 subunits that make up G_i: alpha, beta, and gamma. When activated, the beta and gamma subunits separate from the alpha subunit and bind to potassium channels on the cell membrane thereby triggering an efflux of K^+ out of the cell and hyperpolarizing the cell. This reduces the rate of action potentials and reduces heart rate. Furthermore, the alpha inhibitory subunit binds to AC and inhibits conversion of ATP to cAMP. This reduces pKA levels and consequently reduces the influx of Ca^+, which further slows the frequency of action potentials (Gordon, Gwathmey, & Xie, 2015).

The SNS influences SAN activity by at least 3 mechanisms. The most well-known is by cAMP activation of pKA targeting L-type calcium channels for phosphorylation, which keeps the channels open longer, leading to more available Ca^+ and increased action potential events. There is also evidence that cAMP activates I_f by a mechanism

independent of phosphorylation, involving a direct and rapid interaction with the channels at their cytoplasmic side (DiFrancesco & Tortora, 1991).

In a less direct fashion, ANS input has been related to T-type calcium channels in a study by Mangoni et al., (2006) which showed that mice lacking $Ca_v3.1$ had slowed intrinsic heart rate in the presence of ANS blockade. Without ANS blockade, the reduced heart rate in $Ca_v3.1$ knockout mice was masked. This suggests a complimentary relationship between the SNS and T-type calcium channels.

Changes in autonomic activity are associated with cardiac pathologies such as heart failure and arrhythmias. These abnormalities tend to present early in disease progression and have been shown to predict the development of cardiac dysfunction (Ishise et al., 1998). Quantification of ANS activity in the form of heart rate variability (HRV) as well as sympathetic and vagal tone can be a marker for early-stage arrhythmias (Acharya et al., 2004; Karmakar et al., 2009).

It has been suggested that sympathetic nervous system stimulation could increase $I_{Ca,T}$ which could increase the firing rate of SAN cells. Li et al. (2012) demonstrated that SAN cells from $Ca_v3.2$ knockout mice had significantly increased $I_{Ca,T}$ after treatment with isoproterenol, suggesting that native $Ca_v3.1$ channels could be upregulated by the β-adrenergic system, which is mediated by the cAMP/PKA pathway.

1.4. T-type Calcium Channels

Pacemaker cells in the SAN continuously fire action potentials (electrical impulses), which are conducted through the sinus tissue to the surrounding atrial tissues for impulse spreading to the rest of the heart. The spontaneous firing of action potentials is caused

by the automatic depolarization of the diastolic membrane potential of the pacemaker cells. Ion channels are cell membrane proteins with a central pore which allows the flux of ions, generating ionic currents (Marban et al., 2002). Two key ionic currents that underlie the automatic depolarization in pacemaker cells are the funny current (I_f) and T-type calcium current ($I_{Ca,T}$) (Mangoni et al., 2010).

There are two types of calcium channels in the adult heart. T-type (or transient) calcium channels are activated at a low-voltage (-60 to -50 mV) and inactivate quickly when the cell reaches a threshold potential of approximately -40 to -30 mv. L-type (or long-lasting) calcium channels are activated at high-voltage (-40 mV) and trigger contraction in atrial and ventricular myocytes (Ono & Iijima, 2010). When threshold potential is met, L-type calcium channels open and allow external calcium ions to flow into the cytoplasm. In myocytes, the increase in calcium ion concentration triggers a release of internal calcium stores from the sarcoplasmic reticulum thereby providing the larger quantity of calcium required for muscle contraction to the actin and myosin fibers (Sipido, Carmeliet & van de Werf 1998; Callewaert, 1992).

T-type calcium channels were initially thought to play a minor role in cardiac function because of their transient nature. However, patchclamp investigations revealed two distinct peaks of calcium influx, and the discovery of specific T-type channel blockers in the 1990's revealed that these novel channels played a significant role cardiac automaticity (Nilius, Talavera & Verkhratsky, 2006). It was also proposed that T-type channels could contribute to myocyte contraction, but to a much lesser extent than L-type calcium channels given their very low density in ventricular myocytes, transient activation, and smaller contribution to total calcium influx (Sipido, Carmeliet & van de Werf 1998).

There are three T-type channel isoforms: $Ca_v3.1$ (*CACNA1G*), $Ca_v3.2$ (*CACNA1H*), and $Ca_v3.3$ (*CACNA1I*), which are the pore-forming α subunits of the channels (Iftinca, 2011). T-type calcium channels are more widely expressed in the embryonic developing heart. Of note, the embryonic heart lacks a dedicated pacemaker or SAN. In early prenatal development, all cardiomyocytes display automaticity. In the embryonic myocardium, automaticity can originate at any point of the primary heart tube. As the myocytes mature, there is a loss of this 'diffuse' automaticity (Mangoni & Nargeot, 2008). After birth, T-type calcium channels are no longer found in the myocardium and localize to the SAN, where they are known to play a role in pacemaking (Mizuta, 2005).

In the adult heart, T-type calcium channels are highly expressed in the sinus node pacemaker cells with $Ca_v3.1$ (*Cacna1g*) as the predominant isoform. The activation threshold of T-type Ca^{2+} channels overlap with the pacemaker diastolic potentials (-60 to -50 mV), and the resulting inward Ca^{2+} current contributes to diastolic depolarization, accelerating the firing of the next action potential (Figure 3).

Mice with deletion of the *Cacna1g* gene encoding $Ca_v3.1$ had slowed atrioventricular (AV) conduction, as demonstrated by prolonged PR intervals in ECG under anesthesia, but all other parameters were within normal limits (Mangoni & Nargeot, 2008). After autonomic nervous system (ANS) blockade (with propranolol and atropine), sedated $Ca_v3.1^{-/-}$ mice demonstrated reduced intrinsic heart rate as well as prolonged PR intervals compared to littermate wild-type controls. Telemetric ECG of conscious and unrestrained mice over a 24-hour period showed decreased mean heart rate in *Cacna1g* knockout mice. During short bursts of activity (i.e., when the sympathetic nervous system was very active), this difference was masked (Mangoni & Nargeot, 2008).

Previous work from Mangoni et al. (2006) showed that ablation of $Ca_v3.1$ subunits led to a heart rate reduction and prolonged PQ interval due to AV block. Conversely, mice lacking $Ca_v3.2$ showed no difference in heart rate or ECG morphology compared to their wild-type littermates, neither was there any evidence of cardiac arrhythmias in the transgenic mice (Chen et al., 2003).

While T-type calcium channels are typically absent from the adult heart myocardium, there is evidence that they reappear when the heart is subjected to pathological stress that induces cardiac hypertrophy and heart failure (Vassort, Talavera, and Alvarez, 2006). Yasui et al. (2005) showed that $Ca_v3.1$ mRNA was reduced in a mouse model of cardiac hypertrophy induced by aortic banding, while $Ca_v3.2$ mRNA remained comparable to control.

In another study, hypertrophied cells from the right atrium of rats showed that mRNA expression of both subunits were unchanged, but there was a significantly increased amplitude of T-type calcium current ($I_{Ca,T}$), in the hypertrophied cells (Koyama et al., 2009). This highlights the importance of investigating changes in ion channels at the gene, protein, and current level to better understand mechanisms of action.

Neuron-restrictive silencer factor (NRSF) is a transcriptional repressor contributing to the mature phenotype of cardiac myocytes by repressing fetal cardiac genes, including $Ca_v3.2$. Heart-specific inactivation of NRSF caused dilated cardiomyopathy and increased expression of $Ca_v3.2$ in ventricular cells that led to increased vulnerability to arrhythmias and sudden death (Kuwahara et al., 2003).

There is strong evidence that loss-of-function mutations in $Ca_v1.3$ and $Ca_v3.1$ underlie congenital heart block (CHB) disease (Strandberg et al., 2013), which is

characterized by atrioventricular block and fetal bradycardia. Hu et al. (2004) also reported inhibition of $I_{Ca,L}$ and $I_{Ca,T}$ by maternal antibodies from mothers with CHB-affected children. Marger et al. (2011) further supported this hypothesis and showed that while inactivation of $Ca_v3.1$ channels alone moderately reduced AV conduction, additional inactivation of $Ca_v1.3$ induced severe AV block.

In the context of sex differences, it is interesting to note that cardiomyocytes treated with estradiol downregulated $Ca_v3.2$ mRNA and $I_{Ca,T}$ (Marni et al., 2009). In an animal model, it was shown that ovariectomized rats (with diminished estrogen production) had increased heart rate compared to control and supplementing the ovariectomized rats with estradiol reduced heart rate (Marni et al., 2009).

Epidemiological studies in humans have documented that premenopausal women have reduced incidence of cardiovascular disease (CVD) compared to age-matched men (Wake and Yoshiyama, 2009), and they withstand ischemia/reperfusion injury better than males (Hayward, Kelly, & Collins, 2000). Evidence suggests that sex hormones exert a protective effect, because the incidence and severity of CVD increases significantly in women post menopause, and the prevalence of coronary artery disease (CAD) is greater in young women who had oophorectomy than those with intact ovaries (Parker et al., 2009).

1.5. Cardiac Sodium Channel $Na_v1.5$

Voltage-gated Na^+ channels contribute significantly to the upstroke portion of action potentials in both atrial and ventricular myocytes and also provide the driving force for impulse conduction between two neighboring cells. Voltage-gated Na^+ channels are also

expressed in the peripheral part of the SAN and the surrounding atrial tissues (with $Na_v1.5$, encoded by *SCN5A*, as the predominant isoform), but they are absent from central SAN cells. These channels are critical for the conduction of generated impulses to the outside of the sinus node (Figure 2).

Patients with loss-of-function *SCN5A* mutations exhibit sinus node dysfunction (Chiang et al., 2015). Other mutations in *SCN5A* have been associated with loss of depolarizing current in peripheral SAN cells (Veldkamp et al., 2003). Mice that were heterozygous with *Scn5a* mutations had slowed impulse conduction within the sinus node tissue (Lei et al., 2005). Our recent study demonstrated that Wnt/β-catenin signalling inhibits voltage-gated Na^+ current by suppression of $Na_v1.5$/*Scn5a* expression in cardiomyocytes (Liang et al., 2015), but whether this pathway leads to slowed conduction in the SAN is unknown.

1.6. Wnt/β-catenin Signalling Pathway

The Wnt signalling pathway is highly conserved in the animal kingdom and plays critical roles during embryonic heart development (Cadigan & Nusse, 1997). Wnt ligands are secreted, hydrophobic proteins that bind to cell membrane receptors and activate intracellular signalling cascades that control proliferation, migration, differentiation, apoptosis, and polarity (Blankesteijn et al., 1997; Kwon et al., 2007). Mammals have 19 Wnt genes and 10 receptor (Frizzled, Fz) genes. Co-receptors (such as LRP5/6) are also required for conduction of the Wnt signalling (Haegebarth & Clever, 2009). The study of Wnt signalling has been slow-moving due to their complex set of posttranslational

modifications and interactions involving several highly specialized processing enzymes (Nusse, He, and van Amerongen, 2013).

Wnt signalling can be divided into the canonical β-catenin-dependent pathway, and the noncanonical β-catenin-independent pathways. This study focused on the canonical pathway, which is characterized by the translocation of β-catenin to the nucleus of the cell to regulate canonical Wnt pathway-related gene transcription. Wnt proteins that typically activate the canonical pathway include Wnt1 and Wnt3a (Gessert & Kuhl, 2010).

The Wnt/β-catenin pathway is often described as being in an 'off' or 'on' state (MacDonald & He, 2012). In the 'off' state, Frizzled (Fz) receptors are unoccupied by Wnt, β-catenin is phosphorylated by a 'destruction complex' and is targeted for ubiquitination and degradation by the proteosome (Rao & Kuhl, 2010). The destruction complex is held together by Axin2 and is composed of adenomatous polyposis coli (APC), glycogen synthase kinase (GSK-3β), casein kinase (CK)-1, and β-catenin (Giles, van Es, and Clevers, 2003). In the nucleus, transcription factor T-cell factor/lymphoid enhancer factor (TCF/LEF) inhibits transcription of Wnt-responsive genes (Kikuchi et al., 2011).

The pathway is activated ('on') when Wnt binds to the Fz receptor and co-receptor low-density lipoprotein receptor-related protein (LRP)5/6. Axin2 and dishevelled-1 (Dvl-1) are recruited to the cell membrane, and the destruction complex is undone. The rise in cytosolic β-catenin leads to its translocation into the nucleus where β-catenin partners with TCF/LEF and regulates transcription (MacDonald & He, 2012) (Figure 4).

The most prominent Wnt/β-catenin activators work by inhibiting GSK-3β, and disrupting the β-catenin destruction complex, which allows accumulation of β-catenin in the cytoplasm and subsequent translocation to the nucleus and transcription of Wnt target

genes (Tran & Zheng, 2017). CHIR-99021 (CHIR) is a common inhibitor of GSK-3β and is unique in that it strongly induces the Wnt/β-catenin pathway while demonstrating low cell toxicity (Naujok et al., 2014). In 2015, Liang et al. demonstrated a comparable reduction of $Na_v1.5$ in neonatal rat ventricular myocytes (NRVMs) treated with either Wnt3a (300 ng/ml) or CHIR (3 μM).

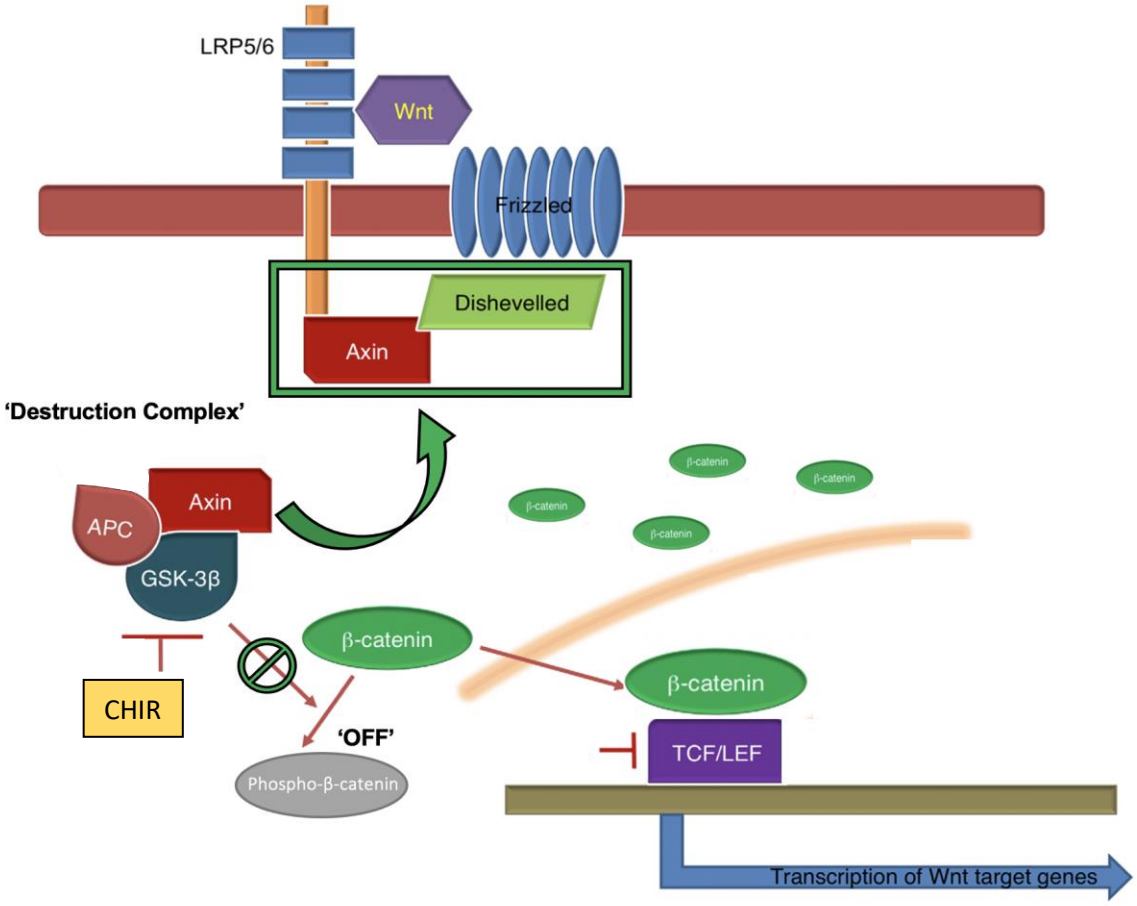

Figure 4: The canonical Wnt pathway (Wnt/β-catenin Pathway). Secreted Wnt proteins bind to the membrane-bound Frizzled receptor (Fzd) and LRP 5/6. Dishevelled then binds to the intracellular domain of Fzd while recruiting Axin from the β-catenin destruction complex, which normally consists of Axin, GSK-3β, and APC. β-catenin accumulates in the cytosol and translocates to the nucleus where it interacts with transcription factors. The small molecule CHIR can quickly enter the cell through passive diffusion and directly inhibit GSK-3β in the destruction complex, also leading to β-catenin accumulation and transcription of Wnt target genes. LRP = lipoprotein-receptor-related protein, APC = adenomatous polyposis coli, TCF/LEF = T-cell factor/lymphoid enhancer-binding factor. Figure adapted from (Tran & Zheng, 2017).

Previous unpublished work from our lab (Figure 5A) suggests that T-type calcium channel gene transcripts are reduced in NRVMs after activation of Wnt/β-catenin signalling. Specifically, RNA sequencing data show reduced mRNA levels of *Cacna1g* (encoding $Ca_v3.1$) in primary culture of neonatal rat ventricular myocytes (NRVMs) after treatment with Wnt3a (300 ug/ml) for 48 hours (n=1) (Figure 5A).

This finding was confirmed with PCR array, which showed reduced *Cacna1g* mRNA in NRVMs treated with Wnt3a (100 ng/ml) or CHIR (3 µM) for 48 hours (n=3, $p<0.01$) compared to control cells treated with DMSO (Figure 5B). In contrast, the L-type calcium channel gene, *Cacna1c*, was not affected (Figure 5A and 5B), suggesting a selective effect of Wnt signalling on the T-type channels.

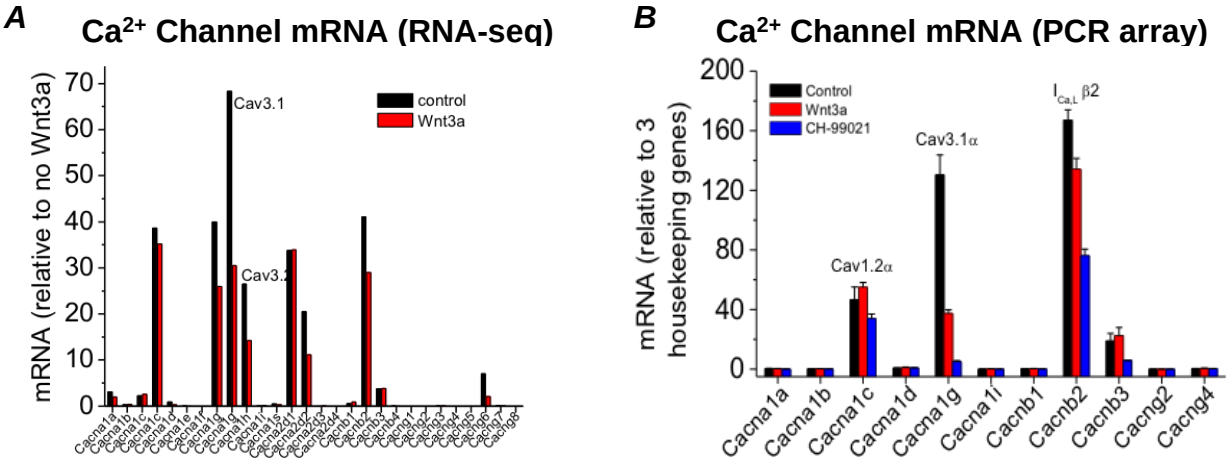

Figure 5: RNA sequencing and PCR array of calcium channel mRNA in cardiomyocytes treated with CHIR or Wnt3a. Previous unpublished work from our lab showing *A*, RNA sequencing data of all cardiac calcium channels, including T-type calcium channel gene *Cacna1g*, in NRVMs after treatment with Wnt3a (100 ng/ml) for 48 hours (n=1). Using a greater sample number (n=3) *B,* PCR array of cardiac-specific calcium channel isoforms revealed a significant reduction in *Cacna1g* after treatment with either Wnt3a (100ng/ml) or CHIR (3 µM) (**p<0.01). There was no significant reduction in L-type calcium channel $Ca_v1.2$ (p=0.741). See full size graph from Figure 5a in Appendix 9.1.

CHIR-99021 (CHIR) is a potent and highly selective inhibitor of GSK-3β (greater than 500-fold selectivity over closely related kinases) that acts as a Wnt/β-catenin pathway activator (Tocris Bioscience, 2021). As a small molecule, CHIR can easily penetrate the cell membrane by simple diffusion whereas Wnt3a first has to bind to its membrane receptor and recruit other signalling proteins before inhibiting the GSK-3β destruction complex. CHIR is also more cost efficient and lasts longer in storage. Therefore, CHIR is used as a pharmacological Wnt/β-catenin activator in this project.

1.6.1. Wnt Signalling in Cardiovascular Disease

Wnt/β-catenin signalling has been shown to regulate, either directly or indirectly, almost every organ system during embryonic development (Komiya & Habas, 2008). Both gain and loss of function mutations of β-catenin are embryonically lethal (Grigoryan et al., 2008). An elaborate pattern of activation and repression of the canonical Wnt pathway critically regulates cardiac morphogenesis (Gessert & Kuhl, 2010; Cohen, Tian, and Morrisey, 2008), but the pathway is typically latent in healthy adult hearts and cardiomyocytes (Cingolani, 2007). Interestingly, a growing body of evidence implicates Wnt/β-catenin signalling in cardiac disease.

Canonical Wnt signalling plays a biphasic role in cardiac development. Activation in early embryonic stem cells induces expression of cardiac genes and differentiation into beating cardiomyocytes (Naito et al., 2006, Ueno et al., 2007). However, the activation of canonical Wnt signalling slightly later in embryonic stem cell differentiation blocks cardiac differentiation, and it has been shown that the deletion of β-catenin in later stage mouse development leads to ectopic heart development along the body axis (Lickert et al., 2002).

These studies suggest that canonical Wnt signalling plays an early positive role in regulating cardiac gene expression in embryonic stem cells and then inhibits cardiac differentiation at a later stage. Given the number of Wnt protein ligands, membrane receptors, and regulators involved in Wnt signalling, the consequences of re-activation in the diseased adult heart are challenging to elucidate.

Antagonism of canonical Wnt signalling can be achieved at different levels of the pathway such as interactions with the expression of GSK3β (Emami et al., 2004), β-catenin (Baurand et al., 2007), or by other ligands that compete with Wnt proteins for binding to the Fz receptor (Saraswati et al., 2010). Given the link between Wnt/β-catenin signalling and reduced ion channel expression previously demonstrated (Liang et al., 2015), it is possible that manipulation of Wnt pathway activity could improve SAN dysfunctions in the context of cardiac disease.

1.6.1.1. Cardiac Hypertrophy

In cardiac hypertrophy, there is an increase in cell size accompanied by protein synthesis, fibrosis, and upregulation of a fetal-gene expression. While initially an adaptive response, cardiac hypertrophy can lead to maladaptive remodeling and heart failure (Rohini et al., 2010). In this state of growth and differentiation, it is not surprising that there are many studies implicating the canonical Wnt pathway in hypertrophic hearts and disease progression. Wnt/β-catenin pathway activity is often measured indirectly via key regulators of the pathway including Dvl-1, β-catenin, and Fz, because the presence of Wnt proteins does not necessarily indicate the ligand is binding Fz receptors and activating the pathway.

In rat models of induced hypertrophy, the Wnt regulator Dvl-1 is increased (Malekar et al., 2010). Transgenic mice overexpressing Dvl-1 have hypertrophic hearts and increased mortality (Malekar et al., 2010). Furthermore, Dvl-1 depleted cardiomyocytes do not develop hypertrophy when treated with isoproterenol (Malekar et al., 2010), and induced hypertrophy is attenuated in Dvl-1 knockout mice (van de Schans et al., 2007).

Dvl-1 is just one of the canonical Wnt pathway-related molecules involved in cardiac hypertrophy. GSK-3β is known to be a negative regulator of hypertrophy and is phosphorylated (inactivated) by most hypertrophic stimuli (Haq et al., 2000; Tateishi et al., 2010; Antos et al., 2002). Conditional overexpression of GSK-3β attenuates hypertrophy development and partially reverses pre-existing hypertrophy in a pressure-overload model (Sanbe et al., 2003). In another study, conditional deletion of β-catenin in cardiomyocytes reduced hypertrophic response (Chen et al., 2006).

1.6.1.2. Myocardial Infarction

When blood flow decreases or stops to a part of the heart due to a mismatch between blood-flow needs and availability, tissue necrosis can occur, referred to as myocardial infarction (MI) (Daskalopoulos et al. 2012). In the early post-MI period (first 3 days), there is an inflammatory response associated with a release of chemokines and cytokines and recruitment of inflammatory cells to aid in removing dead tissue (Daskalopoulos et al. 2012). Fibroblasts then infiltrate the area and are transformed into myofibroblasts. In the late post-MI period (greater than 3 days), myofibroblasts secrete extracellular matrix (ECM) proteins that form scar tissue (Daskalopoulos et al. 2012). Left

ventricular remodeling can occur for many weeks after an event, and large scarring in the MI zone can lead to pathological remodeling and heart failure (Sutton & Sharpe, 2000).

In rats subjected to coronary artery ligation, Dvl-1 was detected in the border zone of the injured tissue 24 hours post-MI, at day 4 expression was also increased in the infarct area, peak expression occurred on day 7, and there were undetectable levels of Dvl-1 by day 28 (Chen et al., 2004). In another study in rats 1-day post-MI, GSK-3β was upregulated in the remote myocardium, and β-catenin was downregulated in the infarct zone (LaFramboise et al., 2005).

Oerlemans et al. (2010) used a transgenic mouse model in which LacZ-positive cells were marked for Axin2 expression, indicating active Wnt signalling. At 7-days post-MI, LacZ+ cells increased by about 50% and more than doubled by days 14 and 21. LacZ+ cells were most prominent in the border zone but were also present in the remote and infarct areas.

Aisagbonhi et al. (2011) also used a transgenic mouse model which expressed β-galactosidase when TCF/LEF transcription in the Wnt pathway were activated by β-catenin signalling. In normal adult mice, Wnt signalling was only in endothelial and smooth muscle cells around large vessels, and in valve mesenchyme. At 4 days post-MI, there was scattered Wnt activation, and at 7-days post-MI, signalling localized to the infarct and peri-infarct area. By 3-weeks post-MI, Wnt signalling was absent.

Interestingly, the cells expressing Wnt activity were mostly fibroblasts with high alpha-smooth muscle actin (α-SMA) expression originating from endothelial cells that had undergone endothelial to mesenchymal transition (EMT) (Aisagbonhi et al., 2011).

Another study revealed that myofibroblasts showed increased expression of FZ2 post-MI (Blankesteijn et al., 1997).

Significantly more research has focused on regulatory mechanisms that influence Wnt/β-catenin signalling than the mechanisms that control Wnt protein processing and secretion from cells, extracellular transportation, or protein reception (Mikels & Nusse, 2006). Thus, while there is evidence suggesting that the reactivation of Wnt signalling in cardiac disease is, at least in part, related to fibroblasts that have undergone EMT in response to cardiac injury (Aisagbonhi et al., 2011), the mechanisms that underlie Wnt protein processing and secretion from these cells have yet to be elucidated.

1.6.1.3. Heart Failure

A fatal end-product of many cardiovascular disorders is heart failure (HF), a progressive disease with a low survival rate (Stewart et al., 2001). MI can result in HF, but less is known about the role of Wnt/β-catenin signalling in other conditions leading to HF (Dawson, Aflaki, and Nattel, 2013). Malekar et al., (2010) showed that cardiac-specific overexpression of Dvl-1 in transgenic mice resulted in hypertrophy, HF, and premature death.

In heart failure there are many different signalling pathways contributing to the net effect, and the Wnt signaling pathway could play various roles depending on the context. For example, some canonical Wnt ligands (i.e., WNT1) are considered anti-apoptotic (Pecina-Slaus, 2010). Antagonism of Wnt signalling [i.e., by secreted frizzled-related proteins (sFRP) 3 and 4] is greatly increased in the failing human heart and seems to be pro-apoptotic (Schumann et al., 2000). Furthermore, GSK-3β activity (a suppressor of

Wnt signalling) is reduced in failing human hearts, and inhibition of GSK-3β protects cells from apoptosis (Haq et al., 2001). Therefore, it is unclear how Wnt/β-catenin signalling contributes to the progression (or prevention) of heart failure.

1.6.1.4. Cardiac Arrhythmias

Arrhythmias refer to any problem with the rate or rhythm of the heartbeat and can occur as a primary condition due to a variety of genetic or environmental factors, but they can also occur as a co-morbidity of other forms of heart disease or injury (Xiao, 2011). There is growing evidence of the role of Wnt/β-catenin signalling in electrical signalling abnormalities. Arrhythmogenic right ventricular cardiomyopathy (ARVC) is a hereditary disease and is a known cause of familial sudden death (Gollob et al., 2011). Mutations in genes encoding Wnt pathway repressors suggest that reduced binding of β-catenin to binding target proteins contributes to ARVC. In that case, the absence of Wnt signalling is associated with arrhythmogenic pathology (Gollob et al., 2011; Garcia-Gras et al., 2006).

Between cardiomyocytes, at gap junctions, there are ion-conducting hemi-channels called connexins (i.e., Cx43, Cx40, and Cx45). Disrupting connexin expression can result in arrhythmia generation and propagation (Dupont et al., 2001). NRVMs treated with the Wnt inhibitor lithium (Li^+) showed increased Cx43 (Ai et al., 2000). A mouse model of cardiomyopathy presented with significant reduction in Cx43 and β-catenin expression. Inducing Wnt signalling led to improved β-catenin/Cx43 colocalization (Ai et al., 2000). This suggests that disturbed Wnt signalling could lead to arrhythmias in diseased hearts.

Interestingly, Wnt8A was associated with atrial fibrillation in a genome-wide association study (Ellinor et al., 2012). Research by Liang et al. in 2015 showed that Wnt/β-catenin signalling in NRVMs reduced expression and activity of cardiac sodium ion channel Nav1.5, which plays a critical role in the fast depolarization phase of the SAN action potential. A number of cardiac diseases are associated with mutations in the gene encoding $Na_v1.5$, including Brugada syndrome (Remme, Brugada, and Brugada, 2006), sick sinus syndrome (SSS) (Benson et al., 2003), and atrial fibrillation (Makiyama et al., 2008).

While it is clear that Wnt signalling plays a role in a variety of cardiac pathologies, there are many potential ligands, receptors, inhibitors, and second messengers that make up a complex system with varying effects depending on cell system, specific ligand/receptor pairings, and temporal organization. This complexity leads to an array of new possibilities for investigations into cardiac pathophysiology and therapeutic targets.

1.7. Research Plan

1.7.1. Rationale

Cardiac arrhythmias are a significant cause of mortality and morbidity. Acquired cardiac arrhythmias are secondary to other common heart disease, such as myocardial infarction and heart failure that are associated with alterations in ion channel expression and/or function. These changes in ion channels are termed “electrical remodeling” and underlie the increased susceptibility to arrhythmias. Understanding the mechanisms for ion channel alterations are critical because it may identify new therapeutic targets.

A growing body of evidence suggests that the embryonically active Wnt/β-catenin pathway is reactivated in adult hearts in the context of heart disease. In cardiomyocytes, this pathway has been shown to decrease Na^+ channels which are known to play a role in impulse conduction in the CCS. Previous work from our lab suggested a decrease in T-type calcium channels in neonatal rat ventricular myocytes after Wnt/β-catenin pathway activation with Wnt3a or CHIR. Reduction of T-type calcium channels could result in abnormal sinoatrial node activity such as slowed beating rate or arrhythmogenic activity.

The impact of Wnt/β-catenin pathway activation on T-type calcium channels in NRVMs will be investigated at the gene and protein level using qPCR and western blot. NRVMs are used as in vitro models for studying mechanisms underlying cardiac pathologies. Compared to adult cardiomyocytes, which do not perform well in culture, NRVMs are relatively easy to culture as monolayers and can be manipulated using molecular and pharmacological tools.

Human induced pluripotent stem cells will also be studied to determine if CHIR-induced changes in T-type calcium channel transcription is species or cell type-specific. Using cells of human lineage will also provide insight into the possible clinical and pharmaceutical relevance. Finally, an in vivo model of Wnt/β-catenin pathway activation will be developed to study changes in cardiac electrophysiology in an animal model. SAN tissue will be collected from these animals for further electrophysiological investigations in ex vivo tissue culture.

Cardiovascular disease (CVD) is the leading cause of death in males and females, but there are biological factors that differ between the sexes (Woodward, 2019). There is a historical bias towards the male model of CVD that may underestimate sex differences,

and research focusing on cardiac differences can help better understand the responsible signalling mechanisms and ensure that therapeutics will work effectively in both men and women. Therefore, in vivo animal experiments will equally represent male and female subjects using sex as a prespecified subgroup analysis.

1.7.2. Hypotheses

- Wnt/β-catenin signalling inhibits T-type Ca^{2+} channels in cardiomyocytes by reducing channel transcript (*Cacna1g* mRNA) and protein ($Ca_v3.1$).
- Activation of Wnt/β-catenin signalling in sinoatrial node (SAN) causes SAN dysfunction by suppressing T-type calcium channels leading to reduced heart rate and by suppressing $Na_v1.5$-mediated sodium channels leading to reduced conduction velocity.

1.7.3. Objectives

This study aims to investigate the effect of Wnt/β-catenin signalling on T-type Ca^{2+} channels in cardiomyocytes, and to investigate the effects of Wnt/β-catenin signalling on sinoatrial node function.

1.7.4. Specific Research Plan

To test the hypothesis, we will undertake the following series of experiments:

1. qRT-PCR of T-type calcium channel gene (*Cacna1g*) abundance in NRVMs treated with CHIR (1 μM, 3 μM, and 10 μM) relative to a control group (DMSO).
2. qRT-PCR of T-type calcium channel gene (*CACNA1G*) in hiPSCs treated with CHIR (10 μM) relative to a control group (DMSO).

3. Western blot analysis of T-type calcium channel protein ($Ca_v3.1$) in NRVMs treated with CHIR (1 μM, 3 μM, and 10 μM) compared to control group (DMSO).
4. Whole-cell patch-clamp of T-type calcium channel current ($I_{Ca,T}$) in NRVMs treated with Wnt3a (300 ng/ml).
5. Activate Wnt/β-catenin signalling in rat hearts using CHIR suspended in a poloxamer gel to compare electrophysiological changes in vivo via electrocardiogram.
6. Develop an ex vivo protocol to maintain SAN tissue harvested from rat hearts and measure intrinsic pacemaker activity via electromyogram.
7. Establish baseline activity of ex vivo SAN tissue and investigate the effect of reduced current in T-type calcium channels or sodium channel $Na_v1.5$ using small molecule inhibitors.
8. Collect SAN tissue from rat hearts 48 hours after activation of Wnt/β-catenin signalling using a poloxamer gel and compare intrinsic pacemaker activity between CHIR and DMSO groups in ex vivo preparations.
9. Investigate molecular mechanisms between Wnt/β-catenin signalling and gene regulation of T-type calcium channels using chromatin immunoprecipitation.

2. Materials and Methods

All animal work was performed with the approval and with accordance of the Animal Care Committee at the University of Ottawa.

2.1. In Vitro Cell Culture Studies

2.1.1. Neonatal rat ventricular myocytes

Neonatal rat ventricular myocytes (NRVMs) were prepared as we previously described (Liang et al., 2015), beginning with trypsin (Amersham Biosciences, Piscataway, NJ) and collagenase (type II, Worthington Biochemical, Freehold, NJ) digestion of ventricles from 2-day-old rats (Sprague-Dawley, Harlan, Charles River, Montreal). Isolated NRVMs were resuspended in M199 medium (Life Technologies) supplemented with 10% fetal bovine serum (FBS) (Gibco), 19.4 mM glucose, 2 mML-glutamine, 2 unit/mL penicillin, 0.8 μg/mL vitamin B12, 10 mM HEPES, and 1× minimal essential media (MEM) nonessential amino acids (Gibco).

Cardiac fibroblasts were removed by two 60-min preplating steps. Cells were plated at 200,000 cells/cm^2 in 6- or 12-well plates (BD Biosciences) precoated with fibronectin (25 μg/ml, Corning) or 0.1% gelatin (StemCell Technologies). FBS in medium was reduced to 2% at day 2 (2 days after plating). For activation of Wnt/β-catenin pathway, recombinant Wnt3a protein (100 ng/ml, R&D systems) or CHIR-99021 (3-10 μM, Selleck Chemicals) was included in the medium starting at day 1 for 48 h.

2.1.2. Human induced pluripotent stem cell-derived cardiomyocytes

Healthy human induced pluripotent stem cells (hiPSCs) (provided by Dr. J.C. Wu Lab) were generated with Sendai virus from peripheral blood mononuclear cells donated

by a healthy volunteer (female, 41-year-old). Differentiation of hiPSCs into cardiomyocytes was performed using a 2-D monolayer protocol in a chemically defined medium (Matsa et al. 2014). Briefly, iPSCs (passage 15-40) at 80-90% confluency were treated with 6 µM CHIR-99021 (Selleck Chemicals) from day 0 to 2 in CDM3 medium (RPMI 1640 supplemented with 213 µg/mL L-ascorbic acid-2-physphate and 500 µg/mL recombinant human albumin).

Cells were maintained from day 2 to 4 in CDM3 medium containing 2 µM Wnt-C59 (Selleck Chemicals). At day 4, cells were cultured in control CDM3 medium (without other added factors) and spontaneous beating cells were usually observed under a microscope at day 7-10. Cells were glucose-starved from day 10 to 14 to purify cardiomyocytes. To minimize well-to-well variations during the differentiation, cells at day 14 were lifted with TrypLE (Life Technologies), pooled, and replated into new plates in CDM3 medium. Cells at day 30-40 of differentiation were used in this study. Healthy hiPSC-derived cardiomyocytes were treated with CHIR (5 µM, Selleck Chemicals Inc.) for 48h before RNA extraction and qRT-PCR studies.

2.1.3. RNA isolation and reverse transcription

After Wnt3a or CHIR treatment, NRVMs and hiPSC-derived cardiomyocytes were collected in RNAprotect Cell Reagent (Qiagen) and stored at -20°C. Total RNA was isolated with RNeasy mini kit (Qiagen) with on-column digestion of genomic DNA with RNase-Free DNase Set (Qiagen). Concentration of RNA in the samples were determined with a NanoDrop 2000 Spectrophotometer (Thermofisher Scientific), and 1000 ng of total RNA was used for cDNA synthesis with a High Capacity cDNA Reverse Transcription Kit

(Applied Biosystems) on a thermocycler (Bio-Rad T100). The cDNA was used for quantitative real-time PCR studies as described below.

2.1.4. Real-time quantitative PCR

Real-time quantitative PCR (qRT-PCR) was performed on a CFX Connect Real-Time PCR Detection System (Bio-Rad) using standard SYBR green method (iTaq Universal SYBR Green Kit; Bio Rad). Primers were designed using Pubmed Primer Blast and synthesized by Life Technologies (Thermofisher Scientific) (Appendix 9.3. - Table 3). Transcript levels of calcium channel genes were normalized to a housekeeping gene (*Hprt1)* in the same samples. Results were analyzed with the $2^{-\Delta\Delta C(t)}$ method and presented as values normalized to control groups in each experiment.

2.1.5. Western blot

NRVMs were homogenized in RIPA buffer containing a protease/phosphatase inhibitor cocktail (Thermofisher Scientific). Protein concentration was determined by BCA assay. Cell lysates (20 µg protein per lane) were run on a 4-12% SDS-polyacrylamide gel and transferred onto a PVDF membrane. The transferred membrane was incubated with rabbit anti-$Ca_v3.1$ antibody (1:200; Alomone Labs) overnight at 4°C, followed by a 2h incubation with a peroxidase-conjugated anti-rabbit secondary antibody (1:2000). Immunoreactivity was detected by chemiluminescence (ECL Western blotting analysis system, Amersham Biosciences). Equal protein loading of the gels was assessed by re-probing the membrane with rabbit anti-calnexin (1:2000,

Abcam). Band densities in western blot experiments were quantified using the “gel analysis tool” of the ImageJ program (Rasband, 2018).

2.1.6. Patch-clamp recording of calcium current

Electrophysiology experiments were carried out using standard whole-cell patch-clamp technique (Liang et al. 2015) with an Axopatch 200B amplifier (Molecular Devices) at a sampling rate of 20 kHz and low-pass Bessel-filtered at 5 kHz. NRVMs, that had been treated with Wnt3a (300 ng/ml) for 48 hours, were placed in a perfusion chamber on the stage of an inverted microscope (IX50, Olympus), and perfused at room temperature with a bath solution (see below). Microelectrodes had tip resistances of 2–5 M MΩ when filled with an internal pipette solution. Ionic currents were recorded in voltage-clamp mode with series resistance compensated by 70–80%. Currents through Ca^{2+} channels were recorded with Ba^{2+} as the charge carrier.

Cells were bathed in a solution containing (in mM): 140 CsCl, 5.4 $BaCl_2$, 2 $MgCl_2$,10 glucose and 10 HEPES, pH=7.4 with CsOH. Pipette solution consisted of (in mM) 5 NaCl, 125 CsF, 10 EGTA, 10 HEPES, 5 Mg-ATP and 0.2 Na-GTP, pH=7.2 with CsOH. Cells were held at −90 mV or −50 mV and a family of voltage steps from −70 mV to +50 mV was applied with 10 mV increments. Currents recorded at a holding potential of −50 mV contained both L-type and T-type Ca^{2+} currents, and currents recorded at −50 mV only contained L-type Ca^{2+} currents.

2.2. In Vivo Animal Studies

2.2.1. Animals

The data presented for the in vivo gel painting procedure (described below) represented results from rats that received identical painting procedures except that the gel contained either DMSO (vehicle) or CHIR (for Wnt activation). The total animal demographics included 8 female (4 former mother rats) and 7 males (1 sample lost at tissue collection step), weighing 150-250g, from 3 to 6 months of age. All rats were Sprague Dawley (Charles River). Surgeries were performed in groups of two, one control (DMSO) and one experimental (CHIR), which were matched for sex, age, and weight. SAN tissue was collected from both rats on the same day and recorded simultaneously within the CO_2 incubator with separate perfusion lines.

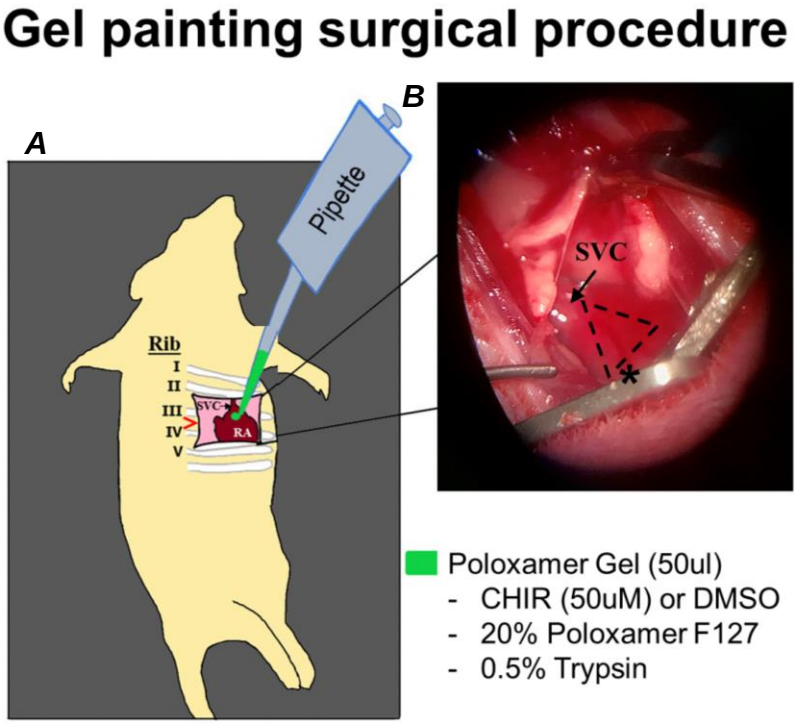

Figure 6: Gel painting surgical technique. *A*, The right side of the heart was exposed by positioning the body at a 45 angle to the left and making an incision between ribs III and IV. *B* The sinoatrial node area (perforated triangle) was identified through a surgical microscope using anatomical landmarks including the superior vena cava, the right atrium, and the sinoatrial node artery. Perforated triangle = sinoatrial node area, * = sinoatrial node artery, SVC = superior vena cava, RA = right atrium.

2.2.2. Surgical Technique

Rats were anesthetized with 3% isoflurane, intubated, transferred to a surgical area, mounted on a heated surgical block, and maintained at 1.5-2% isoflurane. Both legs were taped to the left of the animal's body (Figure 6) for optimal visualization of the right atrium. An incision was made in the left chest at the area of ribs 3 and 4, to access the heart at the level of the superior vena cava, and a retractor was used to separate the ribs and expose the pericardium, which was gently separated with forceps. The right atrium was located through a surgical microscope, and the gel was painted onto the SAN area as described below. The space between the ribs were sutured, the pectoral muscles were placed appropriately, and the incision was closed with staples.

Rats were then transferred to a recovery cage where they were observed for a minimum of four hours before returning to their standard housing. Rats were monitored for 48 hours before sacrifice. All rats recovered within 24 hours without any signs of illness or infection.

2.2.3. "Gel Painting" Protocol

To induce activation of the Wnt signalling in SAN of adult rats, a gel containing CHIR or DMSO (the vehicle) was prepared with a recipe modified from Kikuchi et al. (2005). Briefly, a poloxamer painting solution was prepared one day before painting by adding 20% (wt/vol) poloxamer, and 0.5% (wt/vol) trypsin to PBS and stirred overnight at 4°C. The next day, CHIR (final concentration = 50 µM) or equal volume of DMSO was added to the gel mixture right before painting. The solution was liquid when cold but had a gel-like consistency at physiologic temperature.

After rats were anesthetized as described above, a right thoracotomy was made between the third and fourth left ribs. A 100 ul pipette to was used to deliver two applications of 50 ul gel solution with 5 minutes between for absorption, as described by Kikuchi et al. (2005). The gel was applied to the outer surface of SAN region of the right atrium in rats as identified by anatomical landmarks in vivo (Figure 6), including the superior vena cava and the SAN artery.

2.2.4. In vivo electrocardiogram

Two-lead surface electrocardiogram (ECG) was performed in rats that were anaesthetized with 1.5% isoflurane at one day before surgery (baseline) and 48 hours after surgery (day 2) before heart collection. ECG parameters were analyzed using LabChart Pro (ADInstruments) software and adjusted manually in the averaging view over 3 consecutive 10-second periods. Rats were sacrificed at day two after surgery, and SAN tissues were dissected under a microscope for ex vivo investigation as described below.

2.3. Sinoatrial Node Isolation and Ex Vivo Culture

2.3.1 Experimental design

We also conducted experiments using isolated SAN tissues, because this platform allows direct recording of SAN electrical activities without the influence of autonomic nervous system (e.g., intrinsic heart rate can be recorded). It also allows convenient applications of pharmacological blockers by adding drugs at desired concentrations in the perfusion solution.

After quantifying the effects of Wnt/β-catenin signalling in cells, the plan was to treat isolated SAN tissues with CHIR and continuously record electrical activities for 24 to 48 hours to observe changes in SAN function in real-time as changes in gene transcription took place. However, despite trialing various conditions, ex vivo tissues were only viable for 2 to 9 hours (Fig. 10). This prevented the testing of Wnt/β-catenin signalling applied directly to isolated SAN tissue, because changes in ion channel gene expression would likely take 24 to 48 hours to become measurable.

Furthermore, differences in metabolic activity of cultured cardiac tissues would limit the relevance of results to a physiological context. Therefore, a protocol was developed to apply CHIR directly to the SAN area of rat hearts, allow in vivo incubation for 24 to 48 hours, and then collect SAN tissues for short-term ex vivo recordings comparing intrinsic activity between CHIR and DMSO groups.

Media	**CO_2 (%)**	**O_2 bubbling**	**Temperature (C)**	**System**
Tyrode's Solution*	Low (2.5)	Present	Low (35)	Still
DMEM*	Standard (5)	Absent	Standard (37)	Media change /30 mins
Culture media*	High (7.5)		High (39)	Constant perfusion

**see Appendix 9.2. – Table 2 for media formulations.*

Table 1: Variables for optimizing ex vivo sinoatrial node culture. Baseline conditions were determined using a physiological solution used for langendorff heart perfusion and cell culture: Tyrode's Solution, 5% CO_2, no oxygen bubbling, 35C, and still media. Each variable was then altered systematically and compared between groups in the order as seen below. At each level, the optimal condition was chosen based on 1) most consistent beating rate (SDRR), 2) closest beating rate to physiological range (365 bpm), and 3) longest lasting tissue activity.

2.3.2. Culture conditions

Hearts were collected from control or gel painted rats by thoracotomy under isoflurane. The SAN area was dissected in Tyrode's solution at 35°C based on anatomical landmarks (superior vena cava, right atrium, cristae terminalis, and inferior vena cava). Isolated SAN preparations (Figure 9A) were pinned to silica plates and maintained in a CO_2 incubator at 35°C while being superfused with DMEM (Dulbecco's modified Eagle's medium, Thermo Fisher Scientific) (Figure 7). Extracellular potentials were recorded via two pairs of electrodes that were positioned horizontally and diagonally across a SAN preparation and pinned to the silica dish (Figure 9A). Electrical signals were processed by a BioAmp (AD Instruments) and recorded with LabChart software. Beats were classified as extracellular potentials appearing on both leads more than 2 standard deviations from baseline. Beating rate was averaged over a period of ten minutes.

SAN tissues are very sensitive to temperature, air exposure, media formulation, and stretch. Therefore, we designed a custom constant perfusion system to maintain the tissue in a CO_2 incubator (35°C, 5% CO_2) (Figure 7). Tissue was perfused with a physiological solution (DMEM). Tissue beating rate stabilized within 30 minutes and maintained consistent electrical parameters for a period of at least 2 hours. The average beating rate was 270±22 beats/min, which is comparable to rate reported in other studies of isolation preparations (280±17 beats/min; Morris et al., 2013). Preparations of subsidiary atrial pacemaker tissue have been shown to beat at a rate closer to 185 beats/min (Morris et al., 2013); therefore, our experimental methods provided optimal culturing condition for the central SAN area.

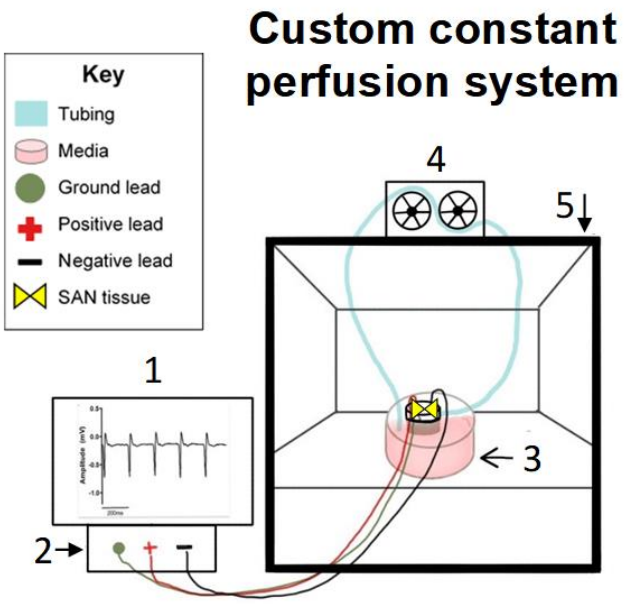

Figure 7: Custom constant perfusion system for ex vivo culture of SAN tissues. A perfusion system was designed to maintain the flow of warm, sterile, physiological solution during ex vivo electrical monitoring. Within a closed CO_2 incubator (**5**), SAN tissue was pinned to a silica plate with electrodes diagonally placed. There was a hole on one end of the plate that allowed media to flow out of the small plate and into a general reservoir (**3**). A tube was inserted into the reservoir and cycled through a peristaltic pump (**4**) back into an opening at the side of the tissue plate. The flow rate was approximately 4 ml/minute. Electrodes were connected to an AD Instruments BioAmp (**2**) and processed through Labchart software (**1**) (actual image of electromyogram data shown in figure).

2.3.3. Small molecule ion channel inhibitors

Control mouse SAN preparations were maintained in a CO_2 incubator at 35°C, and electrical activities were continuously recorded as described above for rat SAN tissues. Effects of blocking T-type Ca^{2+} channels or voltage-gated Na^+ channels were tested by adding to perfusion solution (DMEM) either ML-218 (Tocris Bioscience) (which blocks all $Ca_v3.x$ T-type Ca^{2+} channels; Xiang et al., 2011) at 0, 3, 10 and 30 µM, or Flecainide (Tocris Bioscience) (a blocker of voltage-gated Na^+ channels, IC_{50}=10.7 µM for human $Na_v1.5$; Heath et al., 2011) (at 0, 1, 3, and 10 µM. Changes in beating rate and the width of the beating waves (an index of tissue conduction velocity) after drug applications were analyzed.

2.4. Statistics

Data are expressed as mean ± SEM with $p<0.05$ considered significant. Differences between two means were evaluated by two-tailed Student's t-test. Differences among multiple means were assessed by one-way analysis of variance (ANOVA). When significance was detected by ANOVA, differences among individual means were evaluated *post hoc* by Bonferroni's test. Sub-analysis comparing the effect of treatment group (CHIR or DMSO) and sex (male or female) on average mean beating rate or wave width was performed using two-way ANOVA with results reported as (F value (DFn, DFd)).

3. Results

3.1. Wnt signalling inhibits T-type calcium channels in cardiomyocytes

3.1.1. Wnt/β-catenin signalling reduces T-type calcium channel mRNA and protein levels in cardiomyocytes

RT-qPCR showed a dose-dependent reduction in mRNA levels of *Cacna1g* in NRVMs after 24h treatment with CHIR compared to DMSO (n=7; 1µM, p=0.0387; 3µM, p=0.004; 10µM, p<0.001) (Figure 8A). Human induced pluripotent stem cell (hiPSC)-derived cardiomyocytes treated with 10 µM CHIR for 24h also showed significantly decreased *CACNA1G* compared to the DMSO control group (n=4, p<0.001) (Figure 8D). Importantly, Western blot analysis confirmed a reduction in $Ca_v3.1$ protein in NRVMs treated with CHIR for 48h (n=4; 1 µM, p=0.049; 3 µM, p=0.003; 10 µM, p<0.001) (Figure 8B).

3.1.2. T-type calcium current is reduced in cells treated with Wnt3a

Whole-cell patch-clamp recording showed that T-type calcium current ($I_{Ca,T}$), which is voltage-activated between -60 to -40 mV (Figure 8C), was reduced in NRVMs after treatment with Wnt3a for 48 hours compared to DMSO treatment (n=5 cells, p<0.01).

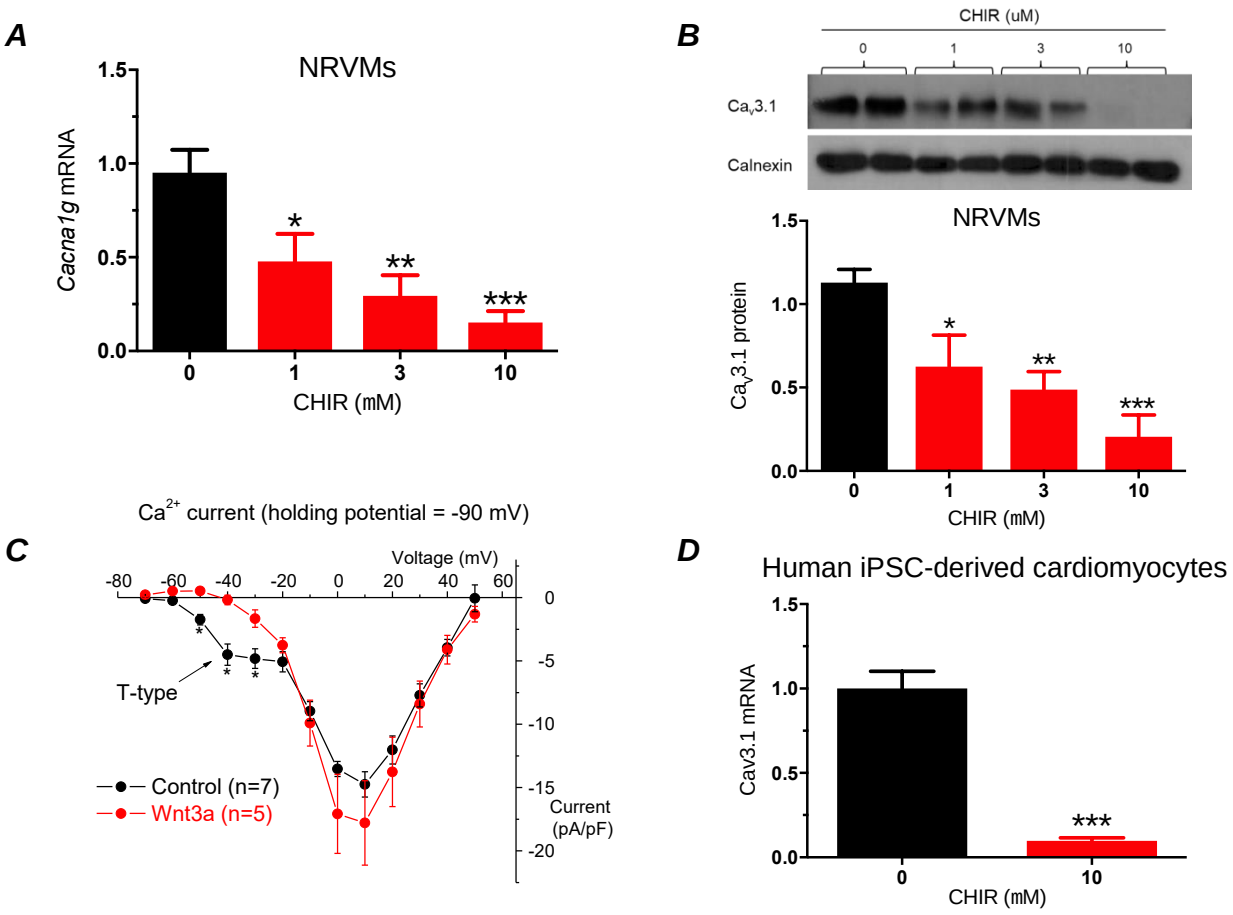

Figure 8: T-type calcium channels in NRVMs or human iPSC-derived cardiomyocytes treated with CHIR or Wnt3a. *A*, RT-qPCR showed a dose-dependent reduction in mRNA levels of *Cacna1g* in NRVMs after 24h treatment with CHIR (n=7; 1 µM *p=0.0387, 3 µM **p=0.004, 10 µM ***p<0.001). *B*, Western blot analysis confirmed a reduction in $Ca_v3.1$ protein in NRVMs treated with CHIR for 48h (n=4; 1 µM *p=0.049, 3 µM **p=0.003, 10 µM ***p<0.001). *C*, T-type calcium current in NRVMs treated with Wnt3a (300 ng/ml) for 48 hours had reduced T-type calcium current (n=5; *p<0.01), which is voltage-activated between -60 to -40mV. *D*, Human induced pluripotent stem cell-derived cardiomyocytes treated with 10 µM CHIR for 24h showed significantly decreased *CACNA1G* mRNA (n=4; ***p<0.001).

3.2. Ex vivo studies of isolated sinoatrial node

3.2.1. Long and short-term culture of sinoatrial node tissues

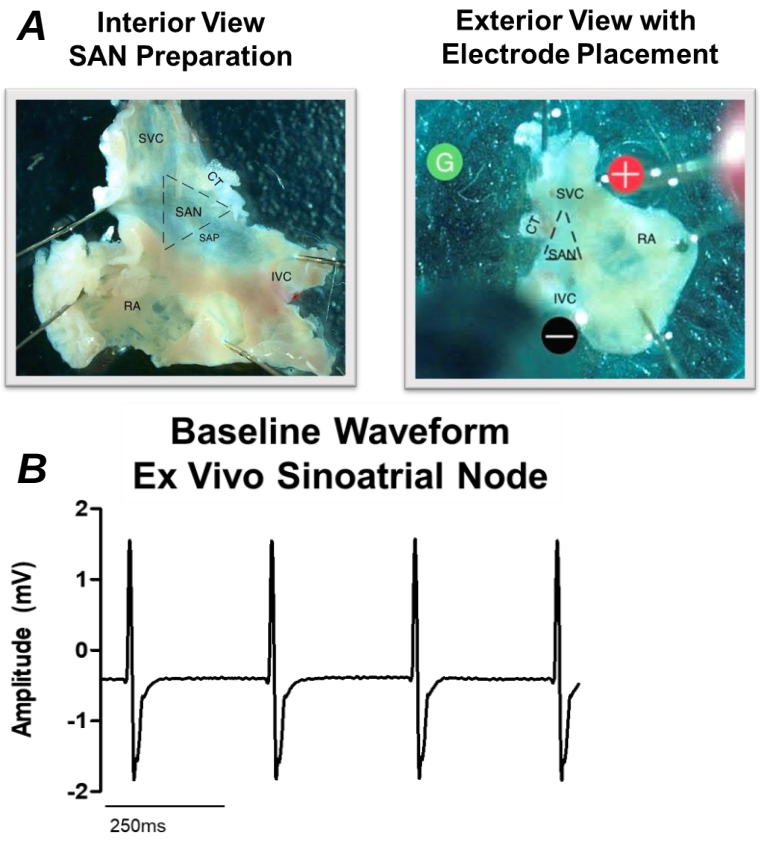

Figure 9: Ex vivo sinoatrial node tissue with electrode placement and sample baseline electrical activity. *A*, Isolated ex vivo sinoatrial node tissue were prepared based on physiological landmarks, and the tissue was pinned to a silica plate. Electrodes were placed diagonally across the tissue (positive + in the upper right and negative - on the lower left). *B*, electrical activity of the tissue (electromyogram) produced a quantifiable waveform with features such as beating rate (BPM), wave duration (ms), and beating rate variability (SDRR). SAN = sinoatrial node, SVC = superior vena cava, CT = cristae terminalis, RA = right atrium, IVC = inferior vena cava, perforated triangle = central sinoatrial node area.

Optimal ex vivo SAN culture conditions were determined by systematically varying each of the factors shown in Table 1. The most stable SAN activity occurred during the first two hours after collection (Figure. 10A). Therefore, we designed an experiment to apply the CHIR treatment (or DMSO as control) in rats and allow incubation for 48h hours before collecting the SAN tissues for ex vivo analysis of intrinsic pacemaker activity.

Three different types of culture solutions were compared, including Tyrode solution, basal cell culture medium (DMEM), and a specially formulated SAN cell culture medium (Sharpe, St. Clair & Proenza, 2016) (full media formulations in Appendix 9.2. – Table 2).

While the SAN cell culture medium performed best in the long term (6+ hours), results were comparable with DMEM in short-term culture (2 hours) (Figure 10a). Tyrode's solution performance was inferior. Therefore, ex vivo experiments were performed using DMEM, as it was sufficient for short-term culture and minimized potential variability of using fetal bovine serum (FBS) (Stein, 2018).

Using a peristaltic pump, tubing, CO_2 incubator and plates, a constant circulation system was developed to perfuse the tissue with physiological solution. Results demonstrated a significant improvement in beating rate and consistency over a 2-hour period in a constant perfusion environment (Figure 10b). This could be explained by the fact that constant circulation of physiological solution more closely resembles in vivo SAN conditions.

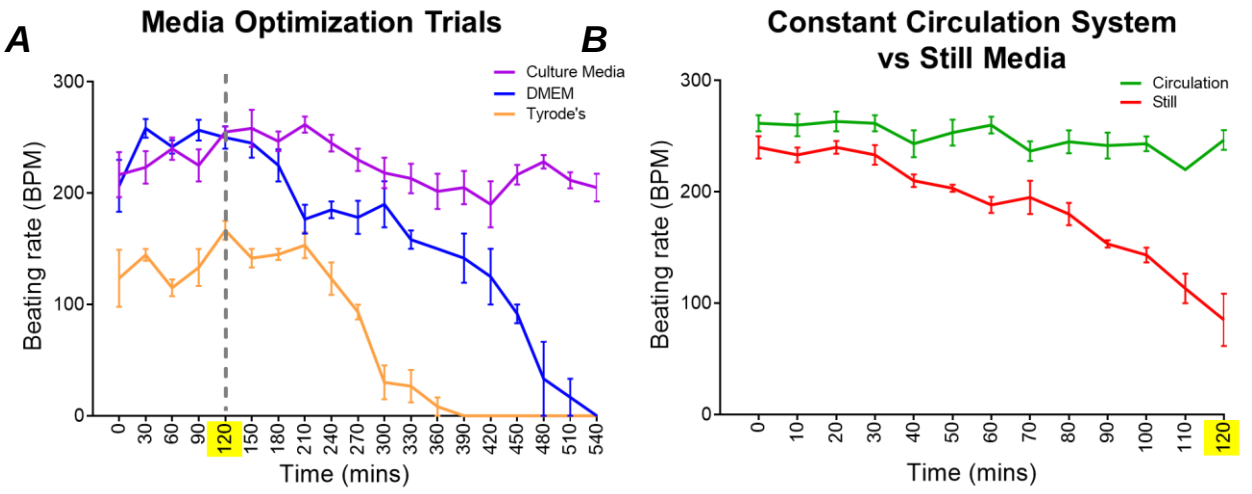

Figure 10. Conditions for ex vivo culture of sinoatrial node tissues. *A*, beating rate of ex vivo SAN preparations (n=2) perfused with one of three different media formulations (Appendix 9.2. – Table 2) over 9 hours. While the culture media performed better in the long term, it was similar to DMEM in short-term culture at 2 hours (green perforated line). *B*, beating rate of control tissue in a CO_2 incubator (35°C, 2.5% CO_2) with still media (DMEM) compared to constant perfusion via a custom circulation system (Figure 6) (n=3).

Other factors investigated in developing the ex vivo protocol included variable temperature settings (high, standard, low), adding a tube to bubble oxygen (with / without), and CO_2 levels (high, standard, low). These factors did not significantly impact tissue activity. Therefore, experimental SAN studies were otherwise conducted under standard cardiomyocyte culture conditions (Xue et al., 2005): 37°C, 5% CO_2, without supplemental oxygen.

3.2.2. Effects of ion channel blockers on SAN function

To test the roles of T-type calcium channels and voltage-gated Na^+ channels in SAN function, pharmacological blockers of these two channels were applied to isolated mouse SAN. ML-218 (a T-type channel blocker) reduced the firing rate of the SAN tissue in a dose-dependent manner but did not alter the length of the impulses (Figure 11 A-D). In contrast, flecainide (a sodium channel blocker) resulted in dose-dependent increases in the impulse duration of individual beats but did not affect the firing rate (Figure 11 E-H). At high doses of flecainide, the SAN began to exhibit conduction block across the tissue (green arrows Figure 11H).

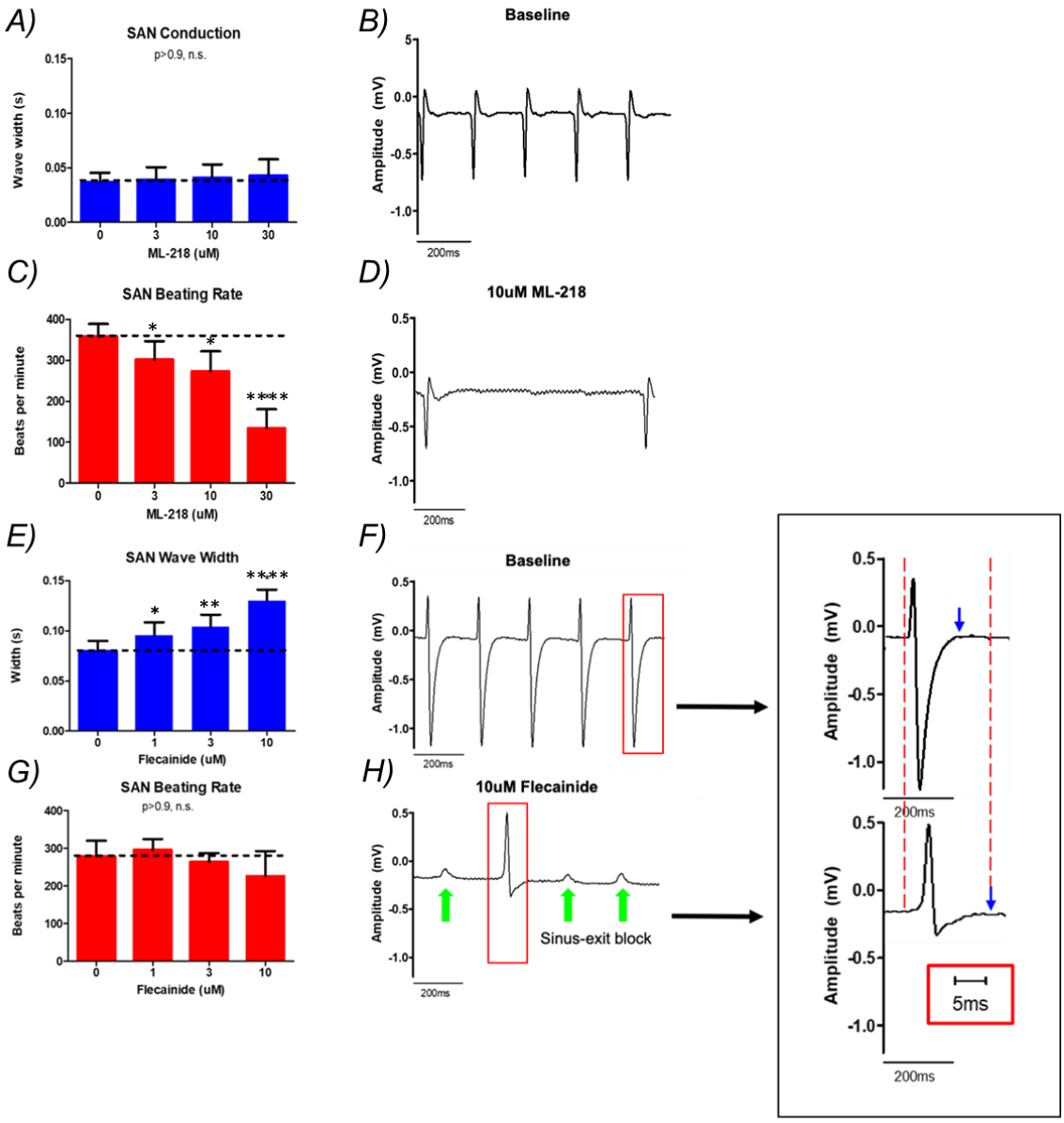

Figure 11. Effects of ion channel blockers on isolated mouse sinoatrial node tissues. Mouse SAN preparations (n=4) were treated with Flecainide, a small molecule inhibitor of sodium channel Nav1.5 or in isolated mouse SAN tissue, perfusion with ML-218 (an $I_{Ca,T}$ blocker) led to dose-dependent reductions in spontaneous beating rate (3μM, *p=0.046; 10μM, *p=0.010; and 30μM, p<0.0001) indicating a critical role of $I_{Ca,T}$ in SAN pacemaking., a specific T-type calcium channel blocker. *A-D* Treatment with ML-218 resulted in decreased beating rate at 3μM (*p=0.046), 10μM (*p=0.010), and 30μM (****p<0.0001) with no impact on wave width 3μM (p=0.721), 10μM (p=0.527), 30μM (p=0.442). *E-H,* Flecainide treatment lengthened wave width (an index of impulse conduction velocity) at 1μM (*p=0.039), 3μM (**p=0.004), and 10μM (****p<0.0001) but did not affect beating rate; 1μM (p=0.452), 3μM (p=0.495), 10μM (p=0.156).

3.3. Effects of Wnt/β-catenin signalling on pacemaker function

3.3.1. In vivo heart rate was not affected by Wnt signalling in SAN

As described in the Methods section, the SAN area of adult rats was painted with a poloxamer gel (20% pluronic F127, 0.5% trypsin, in PBS) containing either CHIR or the vehicle DMSO (n=8). Surface ECG were recorded in isoflurane-anaesthetized rats at one day before surgery (baseline) and at two days after surgery; in our cell culture studies, 48 hours are long enough to see effects of Wnt/β-catenin signalling on Cav3.1 protein and T-type Ca^{2+} current. As shown in Figure 12, there was no in vivo heart rate difference between rats that received CHIR or control (DMSO) gel painting.

3.3.2. Ex vivo heart rate was reduced by Wnt/β-catenin signalling activation in isolated SAN

In order to compare the intrinsic heart rates (i.e., in the absence of active autonomic nervous control) rat SAN tissues were isolated at day 2 after CHIR or DMSO gel painting and maintained in short-term culture as described above. Ex vivo beating rate over a 60-minute period was stable in the CHIR group (p=0.99, F(5,36)=0.1635, n=7^^) and DMSO group (p=0.9874, F(5,36)=0.1187, n=8) as determined by one-way ANOVA (Bartlett's test=5.93, p=0.313). [^^1 CHIR tissue was lost in collection]. However, ex vivo beating rate was lower in the CHIR group (n=7) than in control DMSO group (n=8) as determined by one-way ANOVA (F (1,10) = 16.37).

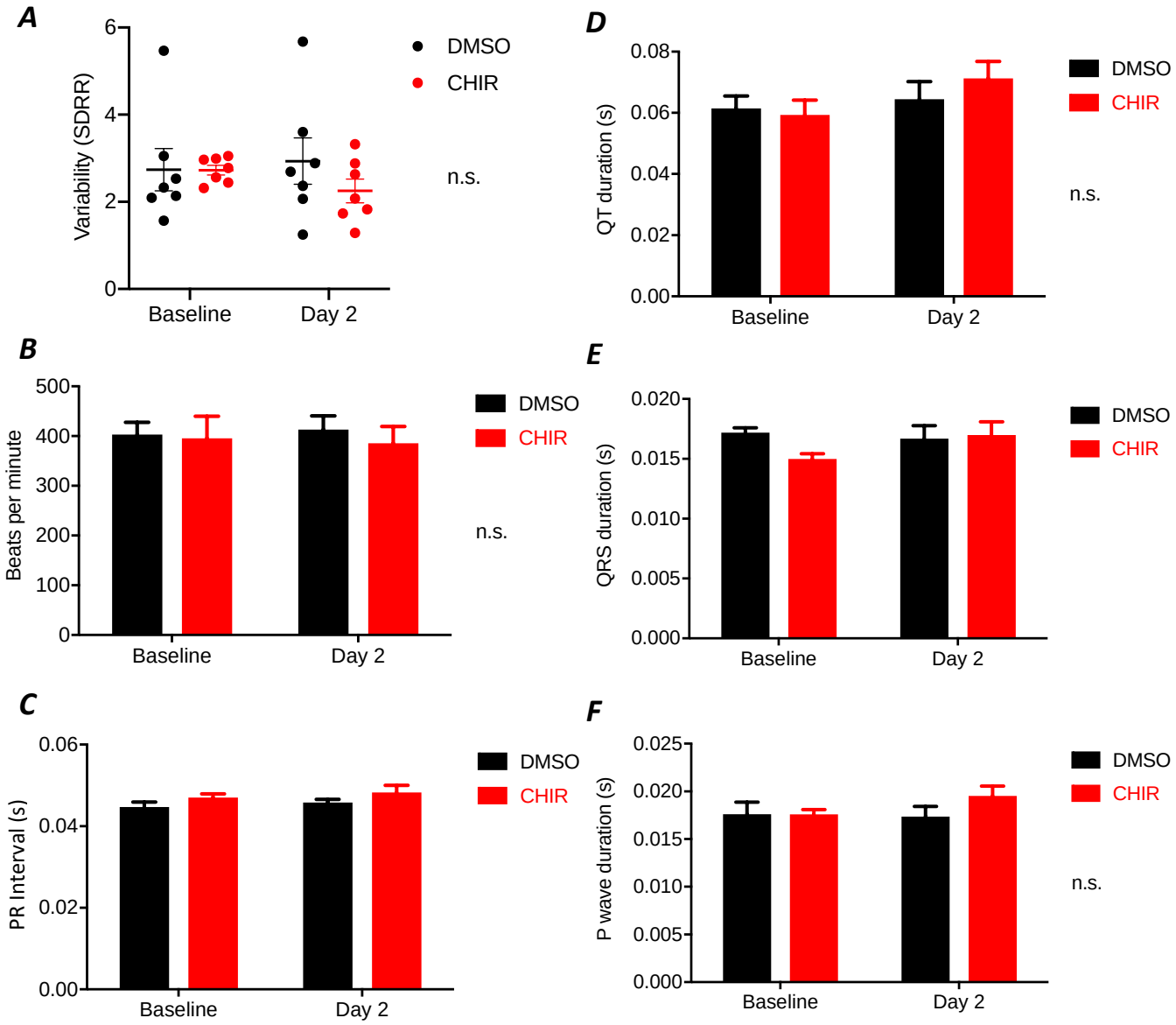

Figure 12: In vivo electrocardiogram parameters before and after CHIR gel painting in rats. There was no significant difference between CHIR or DMSO treatment across all *in vivo* ECG parameters at baseline and day two, respectively: *A*, heart rate variability at baseline (p=0.986, p=0.276); *B*, beating rate (p=0.691, p=0.121); *C*, PR (p=0.150, p=0.849); *D*, QT (p=0.741, p=0.408); *E*, QRS (p=0.053, p=0.901); or *F*, P wave duration (p=0.979, p=0.168) (n=7). Two-tailed paired t-test, df=6. Data in table presented as mean ± SEM. SDRR – standard deviation of R-R intervals.

Consistent with previous findings by our lab that voltage-gated Na^+ channels are inhibited by Wnt signalling (Liang et al., 2015), the width of electrical waves of the SAN tissue (recorded with an ECG system as shown in Figure 9) was significantly increased

in CHIR group (0.083 ± 0.021 seconds, n=7) as compared to DMSO group (0.066 ± 0.022 seconds, n=8) as determined by Student's T-test (p=0.027*).

This indicates a reduced impulse conduction velocity, consistent with a critical role of voltage-gated Na^+ channels in conduction.

3.3.3. Sex does not account for ex vivo differences in CHIR and DMSO groups

Subanalysis of sex differences revealed that the average beating rate for females was 200.8bpm (SEM=31.02, n=8) and for males was 259.5bpm (SEM=19.03, n=7). The average beating rate for females treated with CHIR was 169.8bpm (SEM=5.55, n=4) and DMSO treated females was 231.8 (SEM=10.12, n=4). For male rats, the average beating rate in the CHIR group was 240.5 (SEM=55.28, n=3) and the DMSO group 278.6bpm (SEM=17.59, n=4).

Two-way ANOVA (mixed-effects model due to a missing value for 1 male CHIR subject) comparing the effect of treatment group (CHIR vs. DMSO) and sex (male vs. female) indicated that sex was not a significant factor on average beating rate over the 60 minute period (p=0.1092, F(1,6)=3.533, n=8), assuming sphericity and matching tissue from the same trials. Whereas treatment group (CHIR vs. DMSO) was a significant factor (p=0.0174*, F(1,5)=12.22, n=8) with a mean beating rate of 202.2bpm for CHIR and 255.2bpm for DMSO (difference between means=-52.97, standard error=15.16, Bartlett's test = 1.099)

Similarly, sex did not have a significant effect on wave width (F (1,6) = 0.039, Bartlett's test = 5.93) with averages as follows: DMSO male (0.066 ± 0.008 seconds, n=4),

DMSO female (0.067 ± 0.003ms, n=4), CHIR male (0.081 ± 0.005 seconds, n=3), CHIR female (0.084 ± 0.005 seconds, n=4).

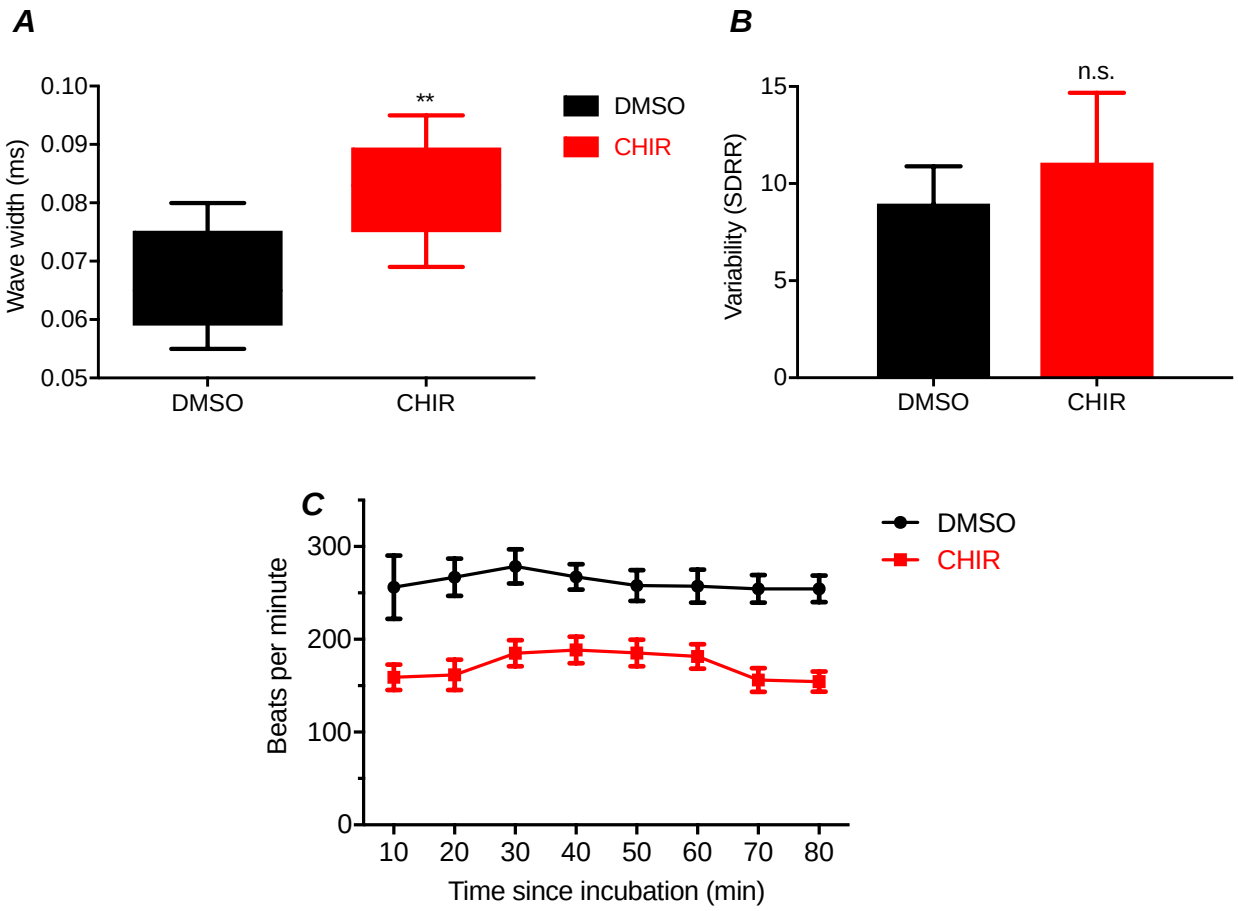

Figure 13. Ex vivo ECG recording of isolated rat SAN demonstrated reduced beating rate in CHIR group. Ex vivo sinoatrial node tissue revealed changes between treatment groups not seen with in vivo recordings. *A*, wave width was reduced in the CHIR treatment group (n=7) compared to DMSO (n=8) (**p=0.003) as determined by Student's T-test. *B*, there was no significant difference in beating rate variability (standard deviation between R-R intervals) between CHIR (n=7) or DMSO (n=9) treatment (p=0.612 n.s.) (T-test). *C,* one-way ANOVA comparing time (F (8,80) = 2.01 n.s.) and treatment showed a significant reduction in average beating rate between the CHIR (199.5 ± 14.6 bpm) versus DMSO-treated group (255.4 ± 8.8 bpm) (**F (1,10) = 16.37).

3.4. Potential mechanisms for Wnt-induced inhibition of the T-type calcium channel: identification of TCF4 binding sites in *Cacna1g* gene promotor

TCF4 is the effector in the Wnt/β-catenin pathway, our lab has previously identified TCF4 binding sites in the sodium channel gene promoter, *Scn5a*, and demonstrated that these TCF4 binding sites are critical for Wnt-mediated suppression of *Scn5a* transcription (Lu et al., 2020). To see similar TCF4 binding sites are also present in the T-type calcium channel gene *Cacna1g* promoter, we have used the multiple sequence alignment tool, ClustalW (Version 2.1; Conway Institute UCD Dublin, 2010) to analyze the *Cacna1g* promoter region. As shown in Figure 14, a consensus binding motif sequence for TCF4 was identified by JASPAR (Fifth expansion; Mathelier et al., 2015). Two putative TCF4 binding sites have been identified in the *Cacna1g* promoter region that are conserved across species, including primate, mouse, and rat (*Homo sapien* reference sequence, GRCh38; *Mus musculus*, GRCm38; *Rattus norvegicus* (Rnor); *Pongo abelli*, PPYG2; and *Macaca mulatta*, Mmul).

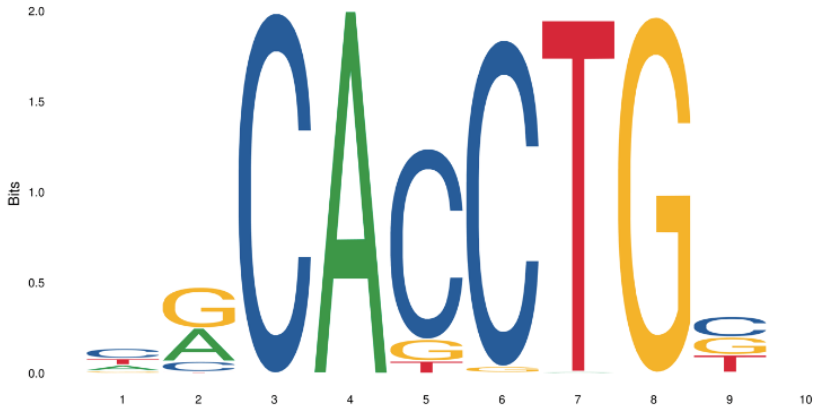

TCF4 Binding Site 1

```
chromosome_GRCh38_17_50559068_      ----------TCTTTTTAATTACCATGACAACAAATCCACACCACCTGGT
chromosome_Mmul_8.0.1_16_38923      ----------TCTCTTTAATTACCATGACAACAAATCCACACCACCTGGT
chromosome_PPYG2_17_41910579_4      ----------TCTCTTTAATTACCATGACAACAAATCCACACCACCTGGT
chromosome_GRCm38_11_94408391_      GGGAGGGGTGTCTCTTCAGTTTCCATGGCAACAAATCCACACCACCTGGT
chromosome_Rnor_6.0_10_8212950      GGG---GGTGTCTCTTCAATCACCATGGCAACAAATCCACACCACCTGGT
```

TCF4 Binding Site 2

```
chromosome_GRCh38_17_50559068_      GCGGAGCCGGGACGATGCTGACCCCTTAGATCCGGCTCCAGCTGCGCCGC
chromosome_Mmul_8.0.1_16_38923      GCGGAGCCGGGACGATGCTGACCCCTTAGATCCGGCTCCAGCTGCGCCGC
chromosome_PPYG2_17_41910579_4      GCGGAGCCGGGACGATGCTGACCCCTTAGATCCGGCTCCAGCTGCGCCGC
chromosome_GRCm38_11_94408391_      GTGGAGCCGGGACGATGCTGACCCCTTAGATCCTGCTCCAGCTGCGCCGA
chromosome_Rnor_6.0_10_8212950      GCGGAGCCGGGACGATGCTGACCCCTTAGATCCTGCTCCAGCTGCGCCGA
```

Figure 14: Multi-sequence alignment of the *Cacna1g* promoter region showing putative binding sites for TCF4, the effector of the Wnt signalling pathway. ClustalW analysis of potential binding sites for the transcription factor TCF4 within the *Cacna1g* promoter region revealed *A*, consensus binding motif sequence logo. *B*, two regions on the *Cacna1g* promoter region were chosen for primer design due to their conservation across primate, mouse, and rat species (homo sapien reference sequence, GRCh38; mus musculus, GRCm38; rattus norvegicus, Rnor; pongo abelli, PPYG2; and macaca mulatta, Mmul).

4. Discussion

4.1. Regulation of cardiac T-type calcium channels in vitro by the Wnt/β-catenin signalling.

The Wnt/β-catenin signalling pathway is preserved in the animal kingdom, and activation of this pathway leads to the translocation of β-catenin from cytosol into the nucleus, where it regulates the transcription of target genes (Cadigan & Nusse, 1997). Recent studies have demonstrated increased nuclear β-catenin levels in cardiomyocytes in cardiac biopsies from patients with ischemic heart failure or dilated cardiomyopathy (Hou et al., 2016). Accordingly, increased levels of Wnt proteins that can activate the β-catenin pathway (e.g., Wnt1, Wnt2 and Wnt4) have been found in animal models of ischemic heart disease (Duan et al., 2012), although the sources of these Wnt proteins are not clear.

Ion channels are proteins that regulate the ion fluxes across the plasma membrane generating ionic currents, which cause cyclic changes in the membrane potentials known as action potentials (Marban et al., 2002). We and other groups have recently demonstrated that Wnt/β-catenin signalling inhibits voltage-gated Na^+ current (I_{Na}) by suppression of the expression of *Scn5a* gene that encodes the I_{Na} pore-forming subunit ($Na_v1.5$) (Liang et al. 2015; Lu et al., 2020; Wang et al., 2016). However, it is not known if other ion channels important for heart function are also regulated by Wnt/β-catenin signalling.

T-type calcium channels ($I_{Ca,T}$) are expressed in fetal and neonatal cardiomyocytes prior to maturation of the cardiac conduction system. In healthy adult

hearts, these channels are exclusively expressed in the cardiac conduction system, including SAN and atrioventricular node (AVN) (Ono & Iijima, 2010). Previous data from our lab with both PCR array and RNA sequencing showed reductions in mRNA of *Cacna1g* (encoding the α subunit of T-type Ca^{2+} channel, $Ca_v3.1$) in NRVMs after treatment with Wnt3a or CHIR (Figure 5). There was no evidence that Wnt signalling effected mRNA levels of *Cacna1c* (encoding the α subunit of L-type Ca^{2+} channel, $Ca_v1.2$), which is consistent with previous studies showing no effects of Wnt3a on $I_{Ca,L}$ amplitude or $Ca_v1.2$ protein level (Liang et al. 2015; Lu et al., 2020; Wang et al., 2016) (Figure 5).

In this study, quantitative real-time PCR (qRT-PCR) and western blot showed dose-dependent reductions in *Cacna1g* mRNA and $Ca_v3.1$ protein level in NRVMs (Figure 8A&B) and in *CACNA1G* mRNA in hiPSCs treated with CHIR (Figure 8D). In addition, whole-cell patch-clamp recording demonstrated reduced $I_{Ca,T}$ amplitude in NRVMs treated Wnt3a, as indicated by the absence of low-voltage (-60 to -40 mV) activated Ca^{2+} current in Wnt3a-treated cells (Figure 8C). These observations suggest that Wnt signalling inhibits $I_{Ca,T}$ by inhibition of *Cacna1g* gene expression in cardiomyocytes.

Reduced T-type calcium channels in the adult heart could lead to disruption of normal cardiac conduction, particularly in the SAN where it is most abundant. Altered ion channel levels (termed electrical remodeling) in heart disease are associated with increased susceptibility to cardiac arrhythmias (Tomaselli & Marban, 1999). It is important to understand the signalling pathways that regulate ion channel expressions in the heart which may provide insights into the mechanisms of electrical remodeling and identify new potential targets for therapy.

4.2. Regulation of sinoatrial node function by the Wnt/β-catenin signalling.

While $I_{Ca,T}$ play a minor role in myocyte contraction, they are critical for the automaticity (i.e., spontaneous firing of action potentials) of the SAN pacemaker cells. The activation threshold of $I_{Ca,T}$ overlaps with the pacemaker diastolic potentials (-60 to -50 mV), so $I_{Ca,T}$ are activated and the resulting inward Ca^{2+} current contributes to diastolic depolarization, accelerating the firing of the next action potential.

In this study, we isolated mouse sinoatrial node (SAN) tissues and maintained them at 37°C with continuously perfusion of a physiological Tyrode solution. Under these conditions, the SAN tissues were able to beat rhythmically for up to 12 hours and their electrical activities were recorded by placing ECG electrodes around SAN tissues. Perfusion of the SAN tissues with ML-218 (a small molecule blocker of $I_{Ca,T}$) reduced their beating rates, consistent with previous studies showing reduced heart rates in mice lacking *Cacna1g* (encoding the T-type Ca^{2+} channel, $Ca_v3.1$) (Mangoni et al., 2006). This suggests that inhibition of $I_{Ca,T}$ reduces the firing rate of the pacemaker tissue.

Given the ability of Wnt signalling to inhibit $I_{Ca,T}$ and the critical role of $I_{Ca,T}$ in SAN pacemaker function, we tested the hypothesis that activation of Wnt signalling leads to SAN dysfunction by inhibiting electrical impulse generation. To induce activation of Wnt signalling, we applied a gel containing CHIR or DMSO (vehicle control) on the outer surface the SAN in mouse heart using the “gel painting” technique, which was designed for application of virus or small molecules to thin layered cardiac tissues (such as atrial tissue and SAN).

In vivo ECG recording at 2 days after “gel painting” showed no difference in heart rates between CHIR and DMSO group (Figure 12B). This is not surprising because

previous studies also showed an unchanged in vivo heart rate in mice lacking the *Cacna1g* gene (encoding Cav3.1) (Mangoni et al., 2006). This may reflect the ability of the mammals to maintain a “normal” heart rate via mechanisms such as the autonomic nervous system. Other parameters of the ECG, such as PR interval, QRS duration, QT interval, were not affected by CHIR painting (Figure 12). This was expected because we only painted CHIR to the SAN region. This also indicates that our surgical procedure was good, and no damage or perturbations to the other parts of the hearts were introduced during the surgery.

Ex vivo preparations revealed that the intrinsic heart rates (i.e., without the effects of autonomic nervous system) in isolated SAN tissues were much lower in the CHIR group (Figure 13C). This suggests that activation of Wnt signalling by CHIR treatment inhibited T-type Ca^{2+} current and reduced intrinsic pacemaker activity, which was masked in vivo likely by alteration in autonomic nervous tones as reported in $Ca_v3.1$ knockout mice (Mangoni et al., 2006). SAN tissue also showed significantly increased wave width in the CHIR group compared to DMSO-treated group. This could be caused by reduced $Na_v1.5$ expression (Liang et al., 2015) in the SAN, which is expected to reduce impulse conduction.

It is important to note that one male CHIR-treated tissue was lost during collection, and so the results for ex vivo groups are unequal (n=7 CHIR and n=8 DMSO), and there was high variability in the CHIR male group (SEM=55.28, n=3) due to an outlier value. The groups were composed of a mix of male and female subjects. A previous study comparing heart function in male and female rats showed no significant difference in intrinsic heart rate between sexes (Schaible & Scheuer, 1984). Indeed, a two-way

ANOVA showed no significant effect of sex, but the subgroup sample size was small (n=4,4,4,3).

Furthermore, in our experiments, approximately 50% of the females were mother rats available after NRVM culture. The mother rats were matched between group, but they had higher weights, and visual inspection during surgery suggested there was more fatty tissue around their hearts than younger control rats. It would be beneficial to include more standard females in future experiments to ensure the validity of the proposed conclusions. The results would have more power with a larger sample size to further investigate possible sex differences.

5. Conclusion

Our results suggest that the Wnt/β-catenin signalling inhibits T-type Ca^{2+} current in cardiomyocytes by, at least partly, reduced *Cacna1g* mRNA and $Ca_V3.1$ protein. Activation of Wnt/β-catenin signalling reduces the intrinsic heart rate likely by inhibition of T-type Ca^{2+} current in sinoatrial node pacemaker cells.

6. Future Directions

Future studies are warranted to investigate the molecular mechanisms of Wnt-induced reductions in *Cacna1g* mRNA, to investigate the effects of Wnt/β-catenin signalling on T-type Ca^{2+} current and action potentials in isolated SAN pacemaker cells, as well as to investigate the role of Wnt/β-catenin signalling in SAN dysfunction in heart disease such as heart failure.

6.1. Elucidate molecular mechanisms underlying Wnt/β-catenin regulation of *Cacna1g*

Our observations that both protein ($Ca_V3.1$) and mRNA (*Cacna1g*) of T-type Ca^{2+} channels were reduced by CHIR suggest regulation of the *Cacna1g* gene by Wnt signalling at the transcriptional level. TCF4 is a key transcription factor that mediates the effects of Wnt/β-catenin pathway on target genes. Our *in silico* analyses have identified a putative TCF4 binding site in the *Cacna1g* promoter region (Fig. 14), which is highly conserved among human, monkeys and rodents. Therefore, future studies are warranted to test the hypothesis that Wnt signalling inhibits *Cacna1g* transcription through TCF4 binding to *Cacna1g* promoter.

First, luciferase promoter reporter assay should be performed to investigate regulation of *Cacna1g* promoter activity by Wnt3a and CHIR. Next, physical binding of TCF4 to the putative binding site in *Cacna1g* promoter can be examined by chromatin immunoprecipitation (ChIP) in Wnt3a- and CHIR-treated NRVMs. Then, CRISPR/Cas9 experiments can be designed to introduce indel (i.e., insertion or deletion) mutations in the TCF4 binding site, which will impair TCF4 binding and is expected to attenuate the inhibitory actions of Wnt3a and CHIR on *Cacna1g* expression. All these techniques, including luciferase assay, ChIP and CRISPR/Cas9, have been used in our lab's recent publication. These studies are expected to elucidate novel mechanisms of Wnt-inhibition of $I_{Ca,T}$ by demonstrating direct suppression of *Cacna1g* promoter by Wnt signalling.

6.2. Wnt/β-catenin signalling on T-type Ca^{2+} current and action potentials in isolated adult SAN cells

This study has demonstrated reduced intrinsic heart rate in isolated rat SAN after CHIR treatment. Future studies are needed to isolate single myocytes from these SAN tissues, and record spontaneous action potentials and $I_{Ca,T}$ using whole-cell patch-clamp technique. Myocytes isolated from CHIR-painted SAN tissues are expected to have a slower firing rate of action potentials associated with reduced rate of diastolic depolarization, as well as reduced amplitude of $I_{Ca,T}$.

These studies are expected to demonstrate that Wnt signalling causes SAN dysfunction by inhibiting $I_{Ca,T}$. In addition, immunohistological studies to show increased nuclear levels of β-catenin in SAN myocytes after CHIR gel painting will be useful to confirm successful activation of the Wnt/β-catenin pathway by CHIR.

6.3. Wnt/β-catenin signalling and SAN dysfunction in clinical models

Our lab has recently generated mice with cardiac-specific knockout (KO) of *Ctnnb1* (encoding β-catenin, the key mediator of Wnt signalling) by breeding $Ctnnb1^{flox/flox}$ mice with αMHC-Cre mice. Sinoatrial node dysfunction can be induced by chronic angiotensin II (Ang II) treatment as described by Dr. Robert Rose's group (Mackasey et al., 2018). Experiments can be designed to examine if Wnt/β-catenin pathway is activated in Ang II-induced SAN dysfunction and if β-catenin KO mice can be protected from SAN dysfunction.

6.4. Telemetric ECG sinoatrial in conscious (unanesthetized) animals

In a *Cacna1g* knockout mouse model (Mangoni & Nargeot, 2008), there was no demonstrable changes in heart rate in mice under anesthesia. However, telemetric ECG showed a decreased mean heart rate over 24-hours. In the present study, we did not have access to the telemetric ECG equipment, which prevented the study of sinoatrial node function of CHIR-painted rats in conscious status. In addition, the isolated SAN was not studied with optical mapping technique that would reveal abnormalities in tissue conduction. Thus, future studies using telemetric ECG and optical mapping would allow more detailed information on the changes in SAN electrophysiology after Wnt pathway activation.

7. References

Acharya, U. R., Kannathal, N., & Krishnan, S. M. (2004). Comprehensive analysis of cardiac health using heart rate signals. *Physiological Measurement, 25*(5), 1139.

Ai, Z., Fischer, A., Spray, D. C., Brown, A. M. C., & Fishman, G. I. (2000). Wnt-1 regulation of connexin43 in cardiac myocytes. *Journal of Clinical Investigation*, 105(2). https://doi.org/10.1172/JCI7798

Aisagbonhi, O., Rai, M., Ryzhov, S., Atria, N., Feoktistov, I., & Hatzopoulos, A. K. (2011). Experimental myocardial infarction triggers canonical Wnt signaling and endothelial-to-mesenchymal transition. *DMM Disease Models and Mechanisms*, 4(4). https://doi.org/10.1242/dmm.006510

Baldesberger, S., Bauersfeld, U., Candinas, R., Seifert, B., Zuber, M., Ritter, M., … Attenhofer Jost, C. H. (2008). Sinus node disease and arrhythmias in the long-term follow-up of former professional cyclists. *European Heart Journal*, 29(1). https://doi.org/10.1093/eurheartj/ehm555

Bassingthwaighte, J., Hunter, P., & Noble, D. (2009). The Cardiac Physiome: perspectives for the future. *Experimental Physiology*, 94(5), 597-605.

Baurand, A., Zelarayan, L., Betney, R., Gehrke, C., Dunger, S., Noack, C., … Bergmann, M. W. (2007). β-catenin downregulation is required for adaptive cardiac remodeling. *Circulation Research*, 100(9). https://doi.org/10.1161/01.RES.0000266605.63681.5a

Benjamin, E. J., Blaha, M. J., Chiuve, S. E., Cushman, M., Das, S. R., Deo, R., …

Muntner, P. (2017). Heart disease and stroke statistics-2017 update: A report from the American Heart Association. *Circulation, 135*(10), e146-e603.
Benson, D. W., Wang, D. W., Dyment, M., Knilans, T. K., Fish, F. A., Strieper, M. J., … George, A. L. (2003). Congenital sick sinus syndrome caused by recessive mutations in the cardiac sodium channel gene (SCN5A). *Journal of Clinical Investigation*, 112(7). https://doi.org/10.1172/jci18062
Boyett, M. R., D'souza, A., Zhang, H., Morris, G. M., Dobrzynski, H., & Monfredi, O. (2013). Viewpoint: Is the resting bradycardia in athletes the result of remodeling of the sinoatrial node rather than high vagal tone? *Journal of Applied Physiology*. https://doi.org/10.1152/japplphysiol.01126.2012
Brugada, R., Brugada, P., & Brugada, J. (2006). Electrocardiogram interpretation and class I blocker challenge in Brugada syndrome. *Journal of Electrocardiology*, 39(4 SUPPL.). https://doi.org/10.1016/j.jelectrocard.2006.05.014
Cadigan, K.M. & Nusse, R. (1997). Wnt signalling: a common theme in animal development. *Genes and Development, 11*:3286-305.
Callewaert, G. (1992). Excitation-contraction coupling in mammalian cardiac cells. Cardiovascular Research. https://doi.org/10.1093/cvr/26.10.923
Catterall, W.A. (2011). Voltage-gated calcium channels*. Cold Spring Harbor perspectives in biology, 3*(8).
Chan, C.S., Chen, Y.C., Chang, S.L., Lin, Y.K., Kao, Y.H., Chen, S.A. and Chen, Y.J. (2018). Heart failure differentially modulates the effects of Ivabradine on the electrical activity of the sinoatrial node and pulmonary veins. *Journal of Cardiac Failure, 24*, 763-772.
Chandler, N. J., Greener, I. D., Tellez, J. O., Inada, S., Musa, H., Molenaar, P., . . . Dobrzynski, H. (2009). Molecular architecture of the human sinus node: insights into the function of the cardiac pacemaker. *Circulation*, 119(12), 1562-1575.
Chandler, N., Aslanidi, O., Buckley, D., Inada, S., Birchall, S., Atkinson, A., … Dobrzynski, H. (2011). Computer Three-Dimensional Anatomical Reconstruction of the Human Sinus Node and a Novel Paranodal Area. *Anatomical Record*, 294(6). https://doi.org/10.1002/ar.21379
Chen, C. C., Lamping, K. G., Nuno, D. W., Barresi, R., Prouty, S. J., Lavoie, J. L., … Campbell, K. P. (2003). Abnormal coronary function in mice deficient in alpha1H T-type Ca2+ channels, Supporting Material. *Science*, 302(5649).
Chen, L., Wu, Q., Guo, F., Xia, B., & Zuo, J. (2004). Expression of Dishevelled-1 in wound healing after acute myocardial infarction: Possible involvement in myofibroblast proliferation and migration. *Journal of Cellular and Molecular Medicine*, 8(2). https://doi.org/10.1111/j.1582-4934.2004.tb00281.x
Chen, X., Shevtsov, S. P., Hsich, E., Cui, L., Haq, S., Aronovitz, M., … Force, T. (2006). The β-Catenin/T-Cell Factor/Lymphocyte Enhancer Factor Signaling Pathway Is Required for Normal and Stress-Induced Cardiac Hypertrophy. *Molecular and Cellular Biology*, 26(12). https://doi.org/10.1128/mcb.02157-05
Chiang, D.Y., Kim, J.J., Valdes, S.O., de la Uz, C., Fan, Y., Orcutt, J., … Miyake, C.Y. (2015). Loss-of-function SCN5A mutations associated with sinus node dysfunction, atrial arrhythmias, and poor pacemaker capture. *Circulation: Arrhythmia Electrophysiology, 8*, 1105-12.
Choudhury, M., Boyett, M. R., & Morris, G. M. (2015). Biology of the sinus node and its

disease. *Arrhythmia and Electrophysiology Review*, 4(1). https://doi.org/10.15420/aer.2015.4.1.28
Choudhury, M., Boyett, M., Kingston, P., Dobrzynski, H., & Morris, G. (2017). Biopacemaking: New Targets and New Mechanisms. *ProQuest Dissertations Publishing*.
Cingolani, O. H. (2007). Cardiac hypertrophy and the Wnt/Frizzled pathway. *Hypertension*. https://doi.org/10.1161/01.HYP.0000255947.79237.61
Cohen, E. D., Tian, Y., & Morrisey, E. E. (2008). Wnt signaling: An essential regulator of cardiovascular differentiation, morphogenesis and progenitor self-renewal. *Development*. https://doi.org/10.1242/dev.016865
Daskalopoulos, E. P., Hermans, K. C. M., Janssen, B. J. A., & Matthijs Blankesteijn, W. (2013). Targeting the Wnt/frizzled signaling pathway after myocardial infarction: A new tool in the therapeutic toolbox? *Trends in Cardiovascular Medicine*. https://doi.org/10.1016/j.tcm.2012.09.010
Dawson, K., Aflaki, M., & Nattel, S. (2013). Role of the Wnt-Frizzled system in cardiac pathophysiology: A rapidly developing, poorly understood area with enormous potential. *Journal of Physiology*. https://doi.org/10.1113/jphysiol.2012.235382
Deb, A. (2014). Cell-cell interaction in the heart via Wnt/beta-catenin pathway after cardiac injury. *Cardiovascular Research*, 102(2), 214-223.doi:10.1093/cvr/cvu054
DiFrancesco, T. & Tortora, P. (1991). Direct activation of cardiac pacemaker channels by intracellular cyclic AMP. *Nature (London)*, 351(6322), 145–147. https://doi.org/10.1038/351145a0
Dobrzynski, H., Li, J., Tellez, J., Greener, I. D., Nikolski, V. P., Wright, S. E., . . . Boyett, M. R. (2005). Computer three-dimensional reconstruction of the sinoatrial node. *Circulation*, 111(7), 846-854.
D'souza, A., Bucchi, A., Johnsen, A. B., Logantha, S. J. R. J., Monfredi, O., Yanni, J., … Boyett, M. R. (2014). Exercise training reduces resting heart rate via downregulation of the funny channel HCN4. *Nature Communications*, 5. https://doi.org/10.1038/ncomms4775
Duan, J., Gherghe, C., Liu, D., Hamlett, E., Srikantha, L., Rodgers, L., … Deb, A. (2012). Wnt1/βcatenin injury response activates the epicardium and cardiac fibroblasts to promote cardiac repair. *EMBO Journal*, 31(2), 429–442.
Duhme, N., Schweizer, P. A., Thomas, D., Becker, R., Schröter, J., Barends, T. R. M., … Koenen, M. (2013). Altered HCN4 channel C-linker interaction is associated with familial tachycardia-bradycardia syndrome and atrial fibrillation. *European Heart Journal*, 34(35). https://doi.org/10.1093/eurheartj/ehs391
Dupont, E., Ko, Y. S., Rothery, S., Coppen, S. R., Baghai, M., Haw, M., & Severs, N. J. (2001). The gap-junctional protein connexin40 is elevated in patients susceptible to postoperative atrial fibrillation. *Circulation*, 103(6). https://doi.org/10.1161/01.CIR.103.6.842
Ellinor, P. T., Lunetta, K. L., Albert, C. M., Glazer, N. L., Ritchie, M. D., Smith, A. V., … Kääb, S. (2012). Meta-analysis identifies six new susceptibility loci for atrial fibrillation. *Nature Genetics*, 44(6). https://doi.org/10.1038/ng.2261
Emami, K. H., Nguyen, C., Ma, H., Kim, D. H., Jeong, K. W., Eguchi, M., … Kahn, M.

(2004). Erratum: A small molecule inhibitor of β-catenin/cyclic AMP response element-binding protein transcription. *Proceedings of the National Academy of Sciences*. https://doi.org/10.1073/pnas.0407571101

Garcia-Gras, E., Lombardi, R., Giocondo, M. J., Willerson, J. T., Schneider, M. D., Khoury, D. S., & Marian, A. J. (2006). Suppression of canonical Wnt/β-catenin signaling by nuclear plakoglobin recapitulates phenotype of arrhythmogenic right ventricular cardiomyopathy. *Journal of Clinical Investigation*, 116(7). https://doi.org/10.1172/JCI27751

Gessert, S., & Kuhl, M. (2010). The multiple phases and faces of Wnt signalling during cardiac differentiation and development. *Circulation Research, 107*(2), 186-199.

Giles, R. H., Van Es, J. H., & Clevers, H. (2003). Caught up in a Wnt storm: Wnt signaling in cancer. *Reviews on Cancer*. https://doi.org/10.1016/S0304-419X(03)00005-2

Gollob, M. H., Blier, L., Brugada, R., Champagne, J., Chauhan, V., Connors, S., … Woo, A. (2011). Recommendations for the use of genetic testing in the clinical evaluation of inherited cardiac arrhythmias associated with sudden cardiac death: Canadian cardiovascular society/Canadian heart rhythm society joint position paper. *Canadian Journal of Cardiology*, 27(2). https://doi.org/10.1016/j.cjca.2010.12.078

Gordan, R., Gwathmey, J. K., & Xie, L. H. (2015). Autonomic and endocrine control of cardiovascular function. *World journal of cardiology*, 7(4), 204–214. https://doi.org/10.4330/wjc.v7.i4.204

Grigoryan, T., Wend, P., Klaus, A., & Birchmeier, W. (2008). Deciphering the function of canonical Wnt signals in development and disease: Conditional loss- and gain-of-function mutations of β-catenin in mice. *Genes and Development*. https://doi.org/10.1101/gad.1686208

Haegebarth, A., & Clevers, H. (2009). Wnt signalling, lgr5, and stem cells in the intestine and skin. *American Journal of Pathology, 174*(3), 715-721.

Haq, S., Choukroun, G., Kang, Z. Bin, Ranu, H., Matsui, T., Rosenzweig, A., … Force, T. (2000). Glycogen synthase kinase-3β is a negative regulator of cardiomyocyte hypertrophy. *Journal of Cell Biology*, 151(1). https://doi.org/10.1083/jcb.151.1.117

Haq, S., Choukroun, G., Lim, H., Tymitz, K. M., Del Monte, F., Gwathmey, J., … Molkentin, J. D. (2001). Differential activation of signal transduction pathways in human hearts with hypertrophy versus advanced heart failure. *Circulation*, 103(5). https://doi.org/10.1161/01.CIR.103.5.670

Haq, S., Michael, A., Andreucci, M., Bhattacharya, K., Dotto, P., Walters, B., … Force, T. (2003). Stabilization of β-catenin by a Wnt-independent mechanism regulates cardiomyocyte growth. *Proceedings of the National Academy of Sciences of the USA, 100*, 4610–4615.

Hayward C.S., Kelly R.P., Collins P. (2000). The roles of gender, the menopause and hormone replacement on cardiovascular function. *Cardiovascular Research*, 46(28–49).

Heath, B., Cui, Y., Worton, S., Lawton, B., Ward, G., Ballini, E., … Mcmahon, N. (2011).

Translation of flecainide- and mexiletine-induced cardiac sodium channel inhibition and ventricular conduction slowing from nonclinical models to clinical. *Journal of Pharmacological and Toxicological Methods*, 63(3), 258–268.
Hesse, M., Kondo, C.S., Clark, R.B., Su, L., Allen, F.L., Geary-Joo, C.T., Kunnathu, S., …Cross, J.C. (2007). Dilated cardiomyopathy is associated with reduced expression of the cardiac sodium channel Scn5a. *Cardiovascular Research, 75*.
Higgins, D., Sievers, F., Dineen, D., & Wilm, A. (2010). Clustal W [Computer Software]. Conway Institute UCD Dublin. Retrieved from www.clustal.org
Hildebrand, M. E., Isope, P., Miyazaki, T., Nakaya, T., Garcia, E., Feltz, A., . . . Snutch, T. P. (2009). Functional coupling between mGluR1 and Cav3.1 T-type calcium channels contributes to parallel fiber-induced fast calcium signalling within Purkinje cell dendritic spines. *Journal of Neuroscience*, 29(31), 9668-9682.
Hou, B., Ye, B., Li, B., Margulies, B., Xu, B., Wang, B., & Li, B. (2016). Transcription Factor 7-like 2 Mediates Canonical Wnt/β-Catenin Signalling and c-Myc Upregulation in Heart Failure. *Circulation: Heart Failure*, 9(6), e003010–e003010.
Hu, K., Qu, Y., Yue, Y., & Boutjdir, M. (2004). Functional basis of sinus bradycardia in congenital heart block. *Circulation Research*, 94(4). https://doi.org/10.1161/01.res.0000121566.01778.06
Iftinca, M. (2011). Neuronal T–type calcium channels: What's new? Iftinca: T–type channel regulation. *Journal of Medicine and Life, 4*(2), 126–138.
Irisawa, H., Brown, H. F., & Giles, W. (1993). Cardiac pacemaking in the sinoatrial node. *Physiological Reviews*. https://doi.org/10.1152/physrev.1993.73.1.197
Ishise, H., Asanoi, H., Ishizaka, S., Joho, S., Kameyama, T., Umeno, K., & Inoue, H. (1998). Time course of sympathovagal imbalance and left ventricular dysfunction in conscious dogs with heart failure. *Journal of Applied Physiology*, *84*(4), 1234.
Jho, E.-h., Zhang, T., Domon, C., Joo, C.-K., Freund, J.-N., & Costantini, F. (2002). Wnt/β-Catenin/Tcf Signalling Induces the Transcription of Axin2, a Negative Regulator of the Signalling Pathway. *Molecular and Cellular Biology*, 22, 1172.
Karmakar, C. K., Khandoker, A. H., Gubbi, J., & Palaniswami, M. (2009). Complex correlation measure: a novel descriptor for Poincaré plot*. Biomedical engineering online, 8*, 17.
Kikuchi, D., Mcdonald, K., Sasano, K., & Donahue, K. (2005). Targeted Modification of Atrial Electrophysiology by Homogeneous Transmural Atrial Gene Transfer. *Circulation*, 111(3), 264–270.
Kikuchi, A., Yamamoto, H., Sato, A., & Matsumoto, S. (2011). New Insights into the Mechanism of Wnt Signaling Pathway Activation. *International Review of Cell and Molecular Biology*, 291. https://doi.org/10.1016/B978-0-12-386035-4.00002-1
Klabunde, R. E. (2012). Cardiovascular Physiology Concepts - Second edition. *Journal of Chemical Information and Modeling*, 53.
Komiya, Y., & Habas, R. (2008). Wnt signal transduction pathways. *Organogenesis*. https://doi.org/10.4161/org.4.2.5851
Koyama, T., Ono, K., Watanabe, H., Ohba, T., Murakami, M., Iino, K., & Ito, H. (2009). Molecular and electrical remodeling of L- And T-type Ca2+ channels in rat right atrium with monocrotaline-induced pulmonary hypertension. *Circulation Journal*, 73(2). https://doi.org/10.1253/circj.CJ-08-0591

Kuwahara, K., Saito, Y., Takano, M., Arai, Y., Yasuno, S., Nakagawa, Y., … Nakao, K. (2003). NRSF regulates the fetal cardiac gene program and maintains normal cardiac structure and function. *EMBO Journal*, 22(23). https://doi.org/10.1093/emboj/cdg601

Kwon, C., Arnold, J., Hsiao, E. C., Taketo, M. M., Conklin, B. R., & Srivastava, D. (2007). Canonical Wnt signaling is a positive regulator of mammalian cardiac progenitors. *Proceedings of the National Academy of Sciences of the United States of America*, 104(26). https://doi.org/10.1073/pnas.0704044104

Laframboise, W. A., Bombach, K. L., Dhir, R. J., Muha, N., Cullen, R. F., Pogozelski, A. R., … Magovern, J. A. (2005). Molecular dynamics of the compensatory response to myocardial infarct. *Journal of Molecular and Cellular Cardiology*, 38(1). https://doi.org/10.1016/j.yjmcc.2004.09.011

Lakatta, E. G., Maltsev, V. A., & Vinogradova, T. M. (2010). A coupled SYSTEM of intracellular Ca2+ clocks and surface membrane voltage clocks controls the timekeeping mechanism of the heart's pacemaker. *Circulation Research, 106*(4).

Lei, M., Jones, S., Liu, J., Lancaster, M., Fung, S., Dobrzynski, H., ··· Boyett, M. (2004). Requirement of neuronal‐ and cardiac‐type sodium channels for murine sinoatrial node pacemaking. *Journal of Physiology*, 559(3), 835–848.

Lei, M., Goddard, C., Liu, J., Léoni, A.L., Royer, A., Fung, S. S.M., … Charpentier, F. (2005). Sinus node dysfunction following targeted disruption of the murine cardiac sodium channel gene Scn5a. *Journal of Physiology, 567*, 387-400.

Lei, M., Zhang, H., Grace, A.A. & Huang, C.L. (2007). SCN5A and sinoatrial node pacemaker function. *Cardiovascular Research, 74*, 356-365.

Li, Y., Wang, F., Zhang, X., Qi, Z., Tang, M., Szeto, C., … Chen, X. (2012). B-Adrenergic stimulation increases Cav3.1 activity in cardiac myocytes through protein kinase A. *PLoS ONE*, 7(7). https://doi.org/10.1371/journal.pone.0039965

Liang, W., Cho, H. C., & Marbán, E. (2015). Wnt signalling suppresses voltage-dependent Na channel expression in postnatal rat cardiomyocytes. *The Journal of Physiology*, *593*(5), 1147-1157.

Lickert, H., Kutsch, S., Kanzler, B., Tamai, Y., Taketo, M. M., & Kemler, R. (2002). Formation of multiple hearts in mice following deletion of β-catenin in the embryonic endoderm. *Developmental Cell*, 3(2). https://doi.org/10.1016/S1534-5807(02)00206-X

Lu, A., Kamkar, M., Chu, C., Wang, J., Gaudet, K., Chen, Y., … Liang, W. (2020). Direct and Indirect Suppression of Scn5a Gene Expression Mediates Cardiac Na+ Channel Inhibition by Wnt Signalling. *Canadian Journal of Cardiology*, 36(4), 564–576.

Lymperopoulos, A., Rengo, G., & Koch, W. J. (2013). Adrenergic nervous system in heart failure: pathophysiology and therapy. *Circulation research*, *113*(6), 739.

MacDonald, B. T., & He, X. (2012). Frizzled and LRP5/6 receptors for Wnt/β-Catenin Signalling. *Cold Spring Harbor Perspectives in Biology, 4*(12), a007880.

Mackasey, M., Egom, E., Jansen, H., Hua, R., Moghtadaei, M., Liu, Y., … Rose, R. (2018). Natriuretic Peptide Receptor-C Protects Against Angiotensin II-Mediated Sinoatrial Node Disease in Mice. JACC: *Basic to Translational Science*, 3(6).

Makiyama, T., Akao, M., Shizuta, S., Doi, T., Nishiyama, K., Oka, Y., … Horie, M.

(2008). A Novel SCN5A Gain-of-Function Mutation M1875T Associated With Familial Atrial Fibrillation. *Journal of the American College of Cardiology*, 52(16). https://doi.org/10.1016/j.jacc.2008.07.013

Malekar, P., Hagenmueller, M., Anyanwu, A., Buss, S., Streit, M.R., Weiss, C.S. …Hardt, S.E. (2010). Wnt signalling is critical for maladaptive cardiac hypertrophy and accelerates myocardial remodeling. *Hypertension, 55*, 939–945.

Maltsev, V.A., Sabbab, H.N., & Undrovinas, A.I. (2002). Down-regulation of sodium current in chronic heart failure: effect of long-term therapy with carvedilol. *Cellular and Molecular Life Sciences, 59*, 1561–1568.

Mangoni, M. E., Traboulsie, A., Leoni, A., Couette, B., Marger, L., Le Quang, K., …Lory, P. (2006). Bradycardia and Slowing of the Atrioventricular Conduction in Mice Lacking $Ca_V3.1/\alpha1G$ T-Type Calcium Channels. *Circulation Research, 98*(11), 1422-1430.

Mangoni, M.E. & Nargeot, J. (2008) Genesis and regulation of the heart automaticity. *Physiology Review*, *88*, 919-982.

Marban, E. (2002). Cardiac channelopathies. *Nature, 415*, 213-218.

Marger, L., Mesirca, P., Alig, J., Torrente, A., Dubel, S., Engeland, B., … Mangoni, M. E. (2011). Functional roles of Cav1.3, Cav3.1 and HCN channels in automaticity of mouse atrioventricular cells: Insights into the atrioventricular pacemaker mechanism. *Channels*, 5(3). https://doi.org/10.4161/chan.5.3.15266

Marni, F., Wang, Y., Morishima, M., Shimaoka, T., Uchino, T., Zheng, M., … Ono, K. (2009). 17β-estradiol modulates expression of low-voltage-activated Ca v3.2 T-type calcium channel via extracellularly regulated kinase pathway in cardiomyocytes. *Endocrinology*, 150(2). https://doi.org/10.1210/en.2008-0645

Mathelier, A., Fornes, O., Arenillas, D.J., Chen, C., Denay, G., Lee, J., …Worsley-Hunt, R. (2015). JASPAR 2016: a major expansion and update of the open-access database of transcription factor binding profiles*. Nucleic Acids Research 2016 44*: D110-D115. Retrieved from http://jaspar.genereg.net

Matsa, E., Burridge, P. W., & Wu, J. C. (2014). Human stem cells for modeling heart disease and for drug discovery. *Science Translational Medicine*. https://doi.org/10.1126/scitranslmed.3008921

Matthijs Blankesteijn, W., Essers-Janssen, Y. P. G., Verluyten, M. J. A., Daemen, M. J. A. P., & Smits, J. F. M. (1997). A homologue of Drosophila tissue polarity gene frizzled is expressed in migrating myofibroblasts in the infarcted rat heart. *Nature Medicine*, 3(5). https://doi.org/10.1038/nm0597-541

Mikels, A. J., & Nusse, R. (2006). Wnts as ligands: Processing, secretion and reception. *Oncogene*. https://doi.org/10.1038/sj.onc.1210053

Milanesi, R., Baruscotti, M., Gnecchi-Ruscone, T., & DiFrancesco, D. (2006). Familial Sinus Bradycardia Associated with a Mutation in the Cardiac Pacemaker Channel. *New England Journal of Medicine*, 354(2). https://doi.org/10.1056/nejmoa052475

Monfredi, O., Dobrzynski, H., Mondal, T., Boyett, M., & Morris, G. (2010). The anatomy and physiology of the sinoatrial node - A contemporary review. *Pacing and Clinical Electrophysiology*, *33*(11), 1392-1406.

Mizuta, E., Miake, J., Yano, S., Furuichi, H., Manabe, K., Sasaki, N., . . . Hisatome, I.

(2005). Subtype switching of T-type Ca 2+ channels from Cav3.2 to Cav3.1 during differentiation of embryonic stem cells to cardiac cell lineage. *Circulation Journal*, 69(10), 1284-1289. doi:10.1253/circj.69.1284

Naito, A. T., Shiojima, I., Akazawa, H., Hidaka, K., Morisaki, T., Kikuchi, A., & Komuro, I. (2006). Developmental stage-specific biphasic roles of Wnt/β-catenin signaling in cardiomyogenesis and hematopoiesis. *Proceedings of the National Academy of Sciences of the United States of America*, 103(52). https://doi.org/10.1073/pnas.0605768103

Naujok, O., Lentes, J., Diekmann, U., Davenport, C., & Lenzen, S. (2014). Cytotoxicity and activation of the Wnt/beta-catenin pathway in mouse embryonic stem cells treated with four GSK3 inhibitors. *BMC Research Notes*, 7(1). https://doi.org/10.1186/1756-0500-7-273

Nilius, B., Talavera, K., & Verkhratsky, A. (2006). T-type calcium channels: The never ending story. *Cell Calcium*, 40(2), 81–88.

Nof, E., Luria, D., Brass, D., Marek, D., Lahat, H., Reznik-Wolf, H., … Glikson, M. (2007). Point mutation in the HCN4 cardiac ion channel pore affecting synthesis, trafficking, and functional expression is associated with familial asymptomatic sinus bradycardia. *Circulation*, 116(5). https://doi.org/10.1161/CIRCULATIONAHA.107.706887

Nusse, R., He, X., & Amerongen, R. V. (2013). Wnt signalling: A subject collection. *Cold Spring Harbor Laboratory Press, 4*(5), a011163.

Nusse, R. & Clevers, H. (2017). Wnt/β-Catenin signalling, disease, and emerging therapeutic Modalities. *Cell*, *169*(6), 985-999.

Ono, K., & Iijima, T. (2010). Cardiac T-type Ca(2+) channels in the heart. *Journal of molecular and cellular cardiology, 48,* 65-70.

Opthof, T., Coronel, R., Rademaker, H.M., Vermeulen, J.T., Wilms-Schopman, F.J., & Janse, M.J. (2000). Changes in sinus node function in a rabbit model of heart failure with ventricular arrhythmias and sudden death. *Circulation, 101*, 2975.

Oerlemans, M.I., Goumans, M.J., van Middelaar, B., Clevers, H., Doevendans, P.A., & Sluijter, J.P. (2010). Active Wnt signalling in response to cardiac injury. *Basic Research in Cardiology, 105*, 631–641.

Park, D.S., & Fishman, G.I. (2011). The cardiac conduction system. *Circulation, 123*(8), 904-915.

Parker W.H., Jacoby V., Shoupe D., Rocca W. (2009). Effect of bilateral oophorectomy on women's long-term health. *Womens Health London England*,5(565–76).

Pećina-Šlaus, N. (2010). Wnt signal transduction pathway and apoptosis: A review. Cancer Cell International. https://doi.org/10.1186/1475-2867-10-22

Rao, T. P., & Kühl, M. (2010). An updated overview on wnt signaling pathways: A prelude for more. *Circulation Research*. https://doi.org/10.1161/CIRCRESAHA.110.219840

Rasband, W.S. (1997-2018). ImageJ [Computer Program]. U.S. National Institutes of Health, Bethesda, Maryland, USA, https://imagej.nih.gov/ij/

Rohini, A., Agrawal, N., Koyani, C. N., & Singh, R. (2010). Molecular targets and regulators of cardiac hypertrophy. *Pharmacological Research*. https://doi.org/10.1016/j.phrs.2009.11.012

Sanbe, A., Gulick, J., Hanks, M. C., Liang, Q., Osinska, H., & Robbins, J. (2003).

Reengineering inducible cardiac-specific transgenesis with an attenuated myosin heavy chain promoter. *Circulation Research*, 92(6). https://doi.org/10.1161/01.RES.0000065442.64694.9F

Saraswati, S., Alfaro, M. P., Thorne, C. A., Atkinson, J., Lee, E., & Young, P. P. (2010). Pyrvinium, a potent small molecule Wnt inhibitor, promotes wound repair and post-MI cardiac remodeling. *PLoS One*, 5(11), e15521.

Schram, G., Pourrier, M., Melnyk, P., & Nattel, S. (2002). Differential distribution of cardiac ion channel expression as a basis for regional specialization in electrical function. *Circulation Research*, 90(9), 939-950.

Shang, L.L., Pfahnl, A.E., Sanyal, S., Jiao, Z., Allen, J., Banach, K. …Dudley, S.C. Jr. (2007). Human heart failure is associated with abnormal C-terminal splicing variants in the cardiac sodium channel. *Circulation Research, 101*, 1146–1154.

Sharpe, E. J., St Clair, J. R., & Proenza, C. (2016). Methods for the Isolation, Culture, and Functional Characterization of Sinoatrial Node Myocytes from Adult Mice. Journal of visualized experiments : *JoVE*, (116), 54555.

Schulze-Bahr, E., Neu, A., Friederich, P., Kaupp, U. B., Breithardt, G., Pongs, O., & Isbrandt, D. (2003). Pacemaker channel dysfunction in a patient with sinus node disease. *Journal of Clinical Investigation*, 111(10). https://doi.org/10.1172/JCI200316387

Schumann, H., Holtz, J., Zerkowski, H. R., & Hatzfeld, M. (2000). Expression of secreted frizzled related proteins 3 and 4 in human ventricular myocardium correlates with apoptosis related gene expression. *Cardiovascular Research*, 45(3). https://doi.org/10.1016/S0008-6363(99)00376-4

Sipido, K. R., Carmeliet, E., & Van De Werf, F. (1998). T-type Ca2+ current as a trigger for Ca2+ release from the sarcoplasmic reticulum in guinea-pig ventricular myocytes. *Journal of Physiology*, 508(2). https://doi.org/10.1111/j.1469-7793.1998.439bq.x

St. John Sutton, M. G., & Sharpe, N. (2000). Left ventricular remodeling after myocardial infarction: Pathophysiology and therapy. *Circulation*, 101(25). https://doi.org/10.1161/01.cir.101.25.2981

Stein, A. (2018). Decreasing variability in your cell culture. *BioTechniques*. https://doi.org/10.2144/000112561

Stewart, S., MacIntyre, K., Hole, D. J., Capewell, S., & McMurray, J. J. V. (2001). More “malignant” than cancer? Five-year survival following a first admission for heart failure. *European Journal of Heart Failure*, 3(3). https://doi.org/10.1016/S1388-9842(00)00141-0

Strandberg, L. S., Cui, X., Rath, A., Liu, J., Silverman, E. D., Liu, X., … Hamilton, R. M. (2013). Congenital Heart Block Maternal Sera Autoantibodies Target an Extracellular Epitope on the α1G T-Type Calcium Channel in Human Fetal Hearts. *PLoS ONE*, 8(9). https://doi.org/10.1371/journal.pone.0072668

Tateishi, A., Matsushita, M., Asai, T., Masuda, Z., Kuriyama, M., Kanki, K., … Matsui, H. (2010). Effect of inhibition of glycogen synthase kinase-3 on cardiac hypertrophy during acute pressure overload. *General Thoracic and Cardiovascular Surgery*, 58(6). https://doi.org/10.1007/s11748-009-0505-2

Tellez, J. O., Dobrzynski, H., Greener, I. D., Graham, G. M., Laing, E., Honjo, H., …

Billeter, R. (2006). Differential expression of ion channel transcripts in atrial muscle and sinoatrial node in rabbit. *Circulation Research*, 99(12). https://doi.org/10.1161/01.RES.0000251717.98379.69
Tocris Bioscience (2021). CHIR 99021. Biological Activity. Retrieved from https://www.tocris.com/products/chir-99021_4423.
Tomaselli, G., & Marbán, E. (1999). Electrophysiological remodeling in hypertrophy and heart failure. *Cardiovascular Research*, *42*(2), 270-83.
Tran, F. H., & Zheng, J. J. (2017). Modulating the wnt signaling pathway with small molecules. *Protein Science*. https://doi.org/10.1002/pro.3122
Ueno, S., Weidinger, G., Osugi, T., Kohn, A. D., Golob, J. L., Pabon, L., … Murry, C. E. (2007). Biphasic role for Wnt/β-catenin signaling in cardiac specification in zebrafish and embryonic stem cells. *Proceedings of the National Academy of Sciences of the United States of America*, 104(23). https://doi.org/10.1073/pnas.0702859104
Valdivia, C.R., Chu, W.W., Pu, J., Foell, J.D., Haworth, R.A., Wolff, M.R., Kamp, T.J., & Makielski, J.C. (2005). Increased late sodium current in myocytes from a canine heart failure model and from failing human heart. *Journal of Molecular and Cellular Cardiology, 38*, 475–483.
Van De Schans, V. A. M., Van Den Borne, S. W. M., Strzelecka, A. E., Janssen, B. J. A., Van Der Velden, J. L. J., Langen, R. C. J., … Blankesteijn, W. M. (2007). Interruption of Wnt signaling attenuates the onset of pressure overload-induced cardiac hypertrophy. *Hypertension*, 49(3). https://doi.org/10.1161/01.HYP.0000255946.55091.24
Vassort, G., Talavera, K., & Alvarez, J. (2006). Role of T-type Ca 2+ channels in the heart. *Cell Calcium*, 40(2), 205–220.
Veldkamp, M. W., Wilders, R., Baartscheer, A., Zegers, J. G., Bezzina, C. R., & Wilde, A. A. (2003). Contribution of sodium channel mutations to bradycardia and sinus node dysfunction in LQT3 families*. Circulation Research*, 92(9), 976-983.
Vidal, M., Cusick, M. E., & Barabasi, A. L. (2011). Interactome networks and human disease. Cell, 144(6), 986-998. doi:10.1016/j.cell.2011.02.016
Wahls S.A. (1985). Sick sinus syndrome*. American Family Physician*, *31*:117–24.
Wake R., Yoshiyama M. (2009) Gender differences in ischemic heart disease. *Recent Patents Cardiovascular Drug Discovery*, 4(234–40).
Wang, N., Huo, R., Cai, B., Lu, Y., Ye, B., Li, X., … Xu, H. (2016). Activation of Wnt/β-catenin signalling by hydrogen peroxide transcriptionally inhibits NaV1.5 expression. *Free Radical Biology and Medicine*, 96, 34–44.
Woodward, M. (2019). Cardiovascular disease and the female disadvantage. *International Journal of Environmental Research and Public Health*. https://doi.org/10.3390/ijerph16071165
Xiao, Y. F. (2011). Cardiac arrhythmia and heart failure: From bench to bedside. *Journal of Geriatric Cardiology.* https://doi.org/10.3724/SP.J.1263.2011.00131
Xiang, Z., Thompson, A., Brogan, J., Schulte, M., Melancon, B., Mi, D., … Xiang, Z. (2011). The Discovery and Characterization of ML218: A Novel, Centrally Active T-Type Calcium Channel Inhibitor with Robust Effects in STN Neurons and in a Rodent Model of Parkinson's Disease. *ACS Chemical Neuroscience*, 2(12), 730.
Xue, T., Cho, H. C., Akar, F. G., Tsang, S. Y., Jones, S. P., Marbán, E., … Li, R. A.

(2005). Functional integration of electrically active cardiac derivatives from genetically engineered human embryonic stem cells with quiescent recipient ventricular cardiomyocytes: Insights into the development of cell-based pacemakers. *Circulation*, 111(1). https://doi.org/10.1161/01.CIR.0000151313.18547.A2

Yanni, J., Tellez, J. O., Sutyagin, P. V., Boyett, M. R., & Dobrzynski, H. (2010). Structural remodelling of the sinoatrial node in obese old rats. *Journal of Molecular and Cellular Cardiology*, 48(4). https://doi.org/10.1016/j.yjmcc.2009.08.023

Yanni, J. O., Tellez, J., Mączewski, M., Mackiewicz, U., Beresewicz, A., Billeter, R., … Boyett, M. (2011). Changes in ion channel gene expression underlying heart failure-induced sinoatrial node dysfunction. *Circulation: Heart Failure, 4*(4), 496.

Yasui, K., Niwa, N., Takemura, H., Opthof, T., Muto, T., Horiba, M., . . . Kodama, I. (2005). Pathophysiological significance of T-type Ca2+ channels: expression of T-type Ca2+ channels in fetal and diseased heart. *Journal of Pharmacological Science*, 99(3).

8. Contributions of Collaborators

The study was designed by the candidate together with the supervisors. The candidate performed the majority of the experiments. Dr. A. Lu helped with the animal surgeries and human iPSC studies. Dr. W. Liang performed PCR array and patch-clamp experiments.

9. Appendices

9.1 Full size graph from Figure 5A

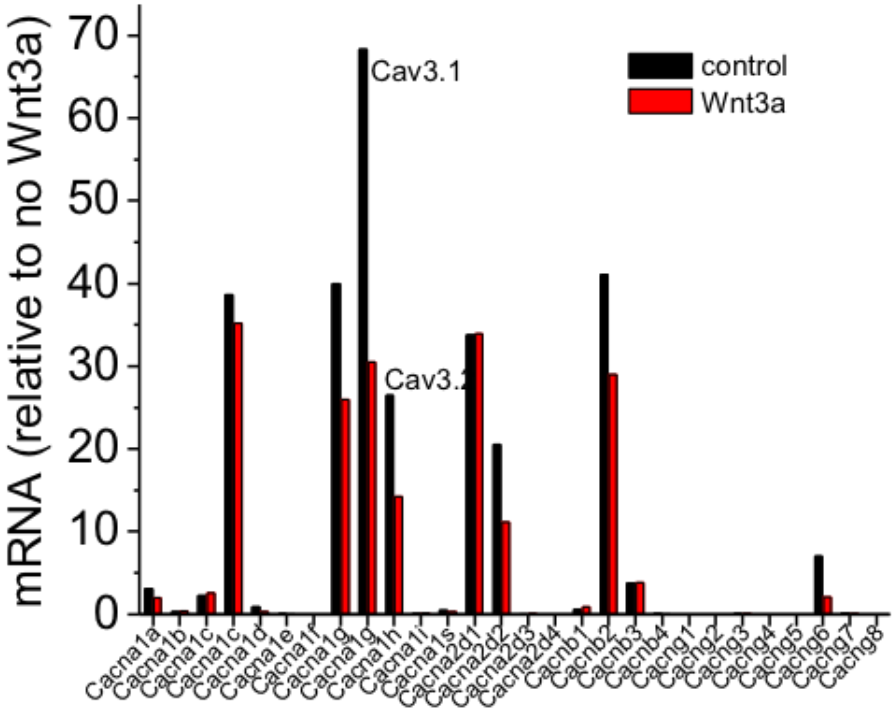

9.2 Media formulations used in ex vivo trials

Component (g/L)	TYRODE'S SOLUTION	DMEM	Culture media
Base	Deionized water	DMEM	Media-199
NaCl	7.9	7	6.8
KCl	0.37	0.31	0.4
CaCl2 · 2H2O	1.8 mL x1M	0.12 (anhydrous)	0.2
MgCl2	1.2 mL x1M	0.048 (anhydrous)	0.098 (anhydrous)
MgSO4	No	0.048 (anhydrous)	No
NaHCO3	No	1.2	2.2
NaH2PO4	No	0.133	0.122 (anhydrous)
HEPES	2.38	3.58	none

Glucose	1.8	3.15 (dextrose)	1
Sodium pyruvate	0.22	0.055	No
BDM	No	No	10mM
Fetal bovine serum	No	No	5%
Insulin	No	No	0.01
Transferrin	No	No	0.0055
Selenium	No	No	0.00001
Penicillin	No	No	0.1U
Streptomyocin	No	No	100
Phenol red	No	0.055	0.0213
Amino acid profile	No	Yes*	Yes**
Vitamin profile	No	Yes*	Yes**

Table 2: Media formulations were trialed in determining optimal conditions for ex vivo sinoatrial node culture. The first media was formulated based on a custom solution, TYRODE'S SOLUTION, used in our lab for short-term (30-60 minutes) langendorff perfusion experiments. The second media was a standard cell culture media, Dulbecco's Modified Eagle Medium (DMEM), formulated by Gibco (Thermo Fisher Scientific). Finally, a media formulation was trialed that was previously described by Sharpe, St Clair, and Proenza (2016) in culturing sinoatrial node myocytes (culture media).

* Full formulation for DMEM: https://www.sigmaaldrich.com/content/dam/sigma-aldrich/docs/Sigma/Product_Information_Sheet/p51445.pdf

** Full formulation for M199: https://www.sigmaaldrich.com/content/dam/sigma-aldrich/docs/Sigma/Formulation/m4530for.pdf

9.3 Primer specifications

Genes		Sequence (5'-3')	Annealing temperature (°C)	Size (bp)
Hprt1	Forward	ACA GGC CAG ACT TTG TTG GA	60	149
	Reverse	TGC CGC TGT CTT TTA GGC TT		
Cacna1g	Forward	GGC TTC CAG GCA GAG GAA AT	60	83
	Reverse	CCC TGA GAG TTG ACA GGC AG		

Table 3: Primer sequences for PCR were designed using Pubmed Primer-BLAST (National Center for Biotechnology Information, Maryland) and synthesized by Life Technologies. As per Bio-Rad specifications, primers were designed within the parameters of 70-150 base pairs long, GC content 40-60%, and melting temperature 50°-65°C.

Binding site, version		Sequence (5'-3')	Annealing temperature (°C)	Size (bp)
1, a	Forward	CCT GCT TCT CTT TCC TTG CAT AAG	60	172
	Reverse	GCA GTA TGT CAC TGT GTG ATG TTC		
1, b	Forward	CTC TTC AAT CAC CAT GGC AAC AAA	60	185
	Reverse	AGG CAA ATC TAG AAC AAC CTG AGT		
2, a	Forward	GAT GCT GAC CCC TTA GAT CCT G	60	187
	Reverse	CTC ACT TTG TTC CGG CTT CTT C		
2, b	Forward	CGA TGC TGA CCC CTT AGA TCC TG	60	197
	Reverse	CGG CTT CCC CTC ACT TTG TTC		

Table 4: Chromatin immunoprecipitation (ChIP) primers for *Cacna1g* were designed using Pubmed Primer-BLAST (National Center for Biotechnology Information, Maryland) based on recommended manufacturer specifications (Cell Signalling Technology, Massachusetts, 2017): 24 nucleotides, melting temperature 60°C, GC content 50%, 150 to 200 base pairs (for standard PCR). Two variations of primers (a / b) were designed for two different binding sites (1 / 2) selected based on compatibility along the *Cacna1g* transcription region based on the identified binding motif (Figure 13). Primers will be validated by standard PCR, and the best for each site will be used for ChIP experiments.